

Intramolecular Hydroalkoxylation/Cyclization of Alkynyl Alcohols Mediated by Lanthanide Catalysts. Scope and Reaction Mechanism

SungYong Seo, Xianghua Yu, and Tobin J. Marks*

Department of Chemistry, Northwestern University, Evanston, Illinois 60208

Received September 12, 2008; E-mail: t-marks@northwestern.edu

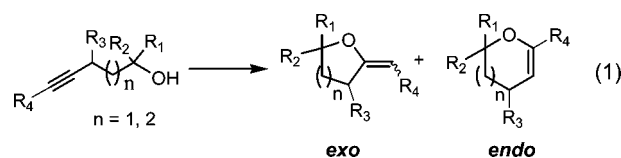
Abstract: Lanthanide–organic complexes of the general type $\text{Ln}[\text{N}(\text{SiMe}_3)_2]_3$ ($\text{Ln} = \text{La}, \text{Sm}, \text{Y}, \text{Lu}$) serve as effective precatalysts for the rapid, exoselective, and highly regioselective intramolecular hydroalkoxylation/cyclization of primary and secondary alkynyl alcohols to yield the corresponding exocyclic enol ethers. Conversions are highly selective with products distinctly different from those generally produced by conventional transition metal catalysts, and turnover frequencies as high as 52.8 h^{-1} at 25°C are observed. The rates of terminal alkynyl alcohol hydroalkoxylation/cyclization are significantly more rapid than those of internal alkynyl alcohols, arguing that steric demands dominate the cyclization transition state. The hydroalkoxylation/cyclization of internal alkynyl alcohols affords excellent *E*-selectivity. The hydroalkoxylation/cyclization of the SiMe_3 -terminated internal alkynyl alcohols reveals interesting product profiles which include the desired exocyclic ether, a SiMe_3 -eliminated exocyclic ether, and the SiMe_3 -O-functionalized substrate. The rate law for alkynyl alcohol hydroalkoxylation/cyclization is first-order in [catalyst] and zero-order in [alkynyl alcohol], as observed in the intramolecular hydroamination/cyclization of aminoalkenes, aminoalkynes, and aminoallenes. An ROH/ROD kinetic isotope effect of 0.95(0.03) is observed for hydroalkoxylation/cyclization. These mechanistic data implicate turnover-limiting insertion of C–C unsaturation into the Ln–O bond, involving a highly organized transition state, with subsequent, rapid Ln–C protonolysis.

Introduction

Oxygen-containing heterocycles are important structural components of a vast array of naturally occurring and pharmacologically active molecules.¹ In this connection, the limitations of traditional heterocycle synthetic methodologies have stimulated considerable interest in developing of new, efficient homogeneous catalytic methods for the synthesis of heterocyclic compounds.² For example, the catalytic addition of alcohols to alkynes represents a direct means for the synthesis of enol ethers and diverse oxygen-containing heterocycles via inter- or intramolecular reaction modes, respectively. Such processes offer great potential from the synthetic point of view because, in principle, addition reactions of this type can be performed with 100% atom efficiency, with negligible waste formation, and for this reason fulfill green chemical requirements more satisfactorily than byproduct-producing substitution reactions leading to the same products.³ Thus, in principle, many important and useful oxygen-containing organic compounds should be acces-

sible via catalytic hydroalkoxylation, and effective intramolecular variants of this reaction would provide straightforward and efficient approaches to numerous oxygen-containing heterocycles. However, while catalytic intramolecular hydroalkoxylation offers many attractions vis-à-vis traditional heterocycle synthetic methodologies, efficient catalytic transformations remain a challenge due to a number of factors, including the relatively large bond enthalpies of typical O–H σ -bonds and the modest reactivity of electron-rich olefins with nucleophiles.

There has therefore been a growing effort to develop more efficient and selective hydroalkoxylation catalysts for this challenging transformation.^{3–6} For intramolecular alkynyl alcohol hydroalkoxylation, there exist two possible products as exemplified by the *exo*- and *endo*-enol ethers shown in eq 1,



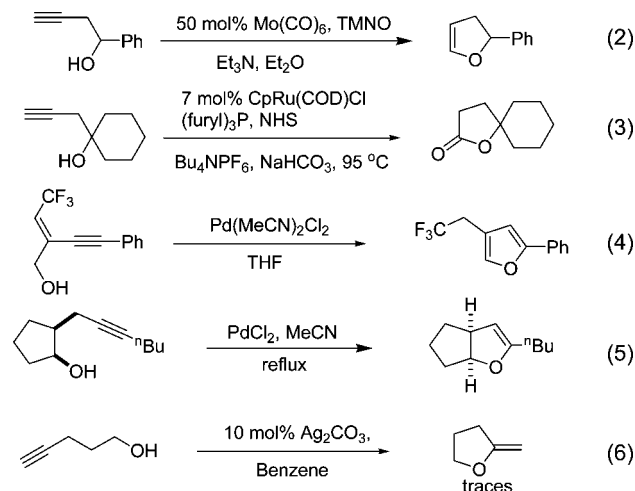
where either *exo*-dig or *endo*-dig cyclization to five- or six-membered rings is allowed according to the Baldwin rules.⁷

- (1) (a) Elliot, M. C.; Williams, E. *J. Chem. Soc., Perkin Trans. 1* **2001**, 2303–2340. (b) Mitchinson, A.; Nadin, A. *J. Chem. Soc., Perkin Trans. 1* **2000**, 2862–2892. (c) Elliot, M. C. *J. Chem. Soc., Perkin Trans. 1* **2000**, 1291–1318. (d) Boivin, T. L. B. *Tetrahedron* **1987**, *43*, 3309–3362.
- (2) (a) Zhang, Z.; Liu, C.; Kinder, R. E.; Han, X.; Qian, H.; Widenhofer, R. A. *J. Am. Chem. Soc.* **2006**, *128*, 9066–9073. (b) Cox, E. D.; Cook, J. M. *Chem. Rev.* **1995**, *95*, 1797–1842. (c) Larcock, R. C.; Leong, W. W. In *Comprehensive Organic Synthesis*; Trost, B. M., Fleming, I., Eds.; Pergamon: New York, Vol 4, 1991. (d) Bird, C. W.; Cheeseman, G. W. H. In *Comprehensive Heterocyclic Chemistry*; Katrinsky, A. R., Rees, C. W., Eds.; Pergamon Press: Oxford, 1984; Vol 4, pp 89–154.

- (3) (a) Alonso, F.; Beletsaya, I. P.; Yus, M. *Chem. Rev.* **2004**, *104*, 3079–3159. (b) Tius, M. A. In *Modern Allene Chemistry*; Krause, N., Hashmi, A. S. K., Eds.; Wiley-VCH: Weinheim, Vol 2, 2004; pp 834–838. (c) Tani, K.; Kataoka, Y. In *Catalytic Heterofunctionalization*; Togni, A., Grützmacher, H., Eds.; Wiley-VCH: Weinheim, 2001; pp 171–216. (d) Bartlett, P. A. In *Asymmetric Synthesis*; Morrison, J. D., Eds.; Academic Press: New York, 1984; Vol. 3, p 455.

The cycloisomerization of alkynyl alcohols to endocyclic enol ethers via metal vinylidenes was first introduced by McDonald's group.^{5h} Here Mo(CO)₆^{5k} and W(CO)₆⁸ are employed to form a metal vinylidene intermediate which subsequently generates the isomerized endocyclic ether (e.g., eq 2). Trost's and Vatile's groups used CpRu(COD)Cl⁹ and Pd(MeCN)₂ClNO₂¹⁰ catalysts to produce γ -lactones via intramolecular hydroalkoxylation and oxidation (eq 3), while Qing, et al. have studied cycloisomerizations mediated by Pd(MeCN)₂Cl₂ (e.g., eq 4).¹¹ With regard to accessing exocyclic enol ethers, there are two different types of reaction products derived from either no isomerization or isomerization, following intramolecular hydroalkoxylation. The first successful demonstration of such cycloisomerizations employed PdCl₂ as the catalyst in refluxing MeCN (e.g., eq 5),¹² after which, other Pd catalysts such as Pd(OAc)₂,¹³ K₂PdI₄,¹⁴ and Ru(PPh₃)(*p*-cymene)Cl₂¹⁵ were developed. The first example of intramolecular hydroalkoxylation not accompanied by isomerization was reported by Villemin using HgO and BF₃·Et₂O.¹⁶ Similar transformations were subsequently reported using Pd(OAc)₂¹⁷ and Ag₂CO₃ (e.g., eq 6).^{5e,18}

Organolanthanide complexes are known to be highly active hydrofunctionalization catalysts.^{19–21} Among these catalysts, homoleptic Ln[N(SiMe₃)₂]₃ amido complexes (Ln = lanthanide,

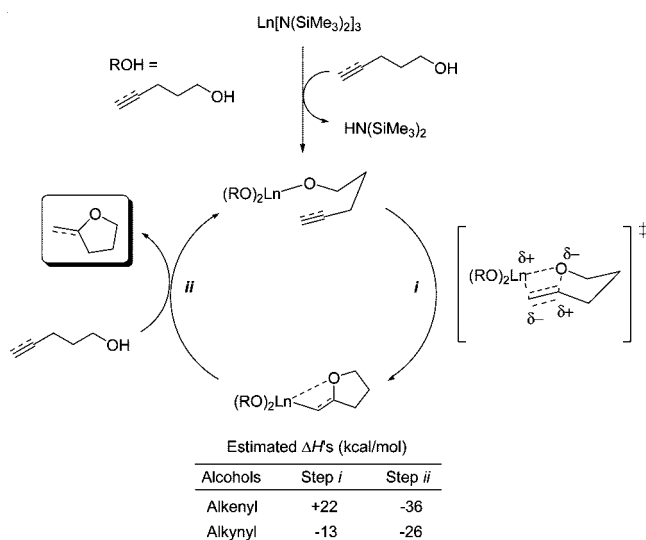


Y) are versatile agents for a variety of organic transformations, which can be either intermolecular or intramolecular in character. Successful intermolecular transformations include the synthesis of ynones,²² cross-Aldol reactions,²³ coupling reactions of isocyanides with terminal alkynes,²⁴ dimerization of terminal alkynes,²⁵ guanylation of amines,²⁶ hydrosilylation,²⁷ hydroboration,²⁸ Tishchenko aldehyde dimerization,²⁹ and amidations.³⁰ Intramolecular transformations include hydroelementation processes, such as hydroamination,^{31,29b} hydrophosphination,^{20b} and hydroalkoxylation.³²

- (4) For examples of alkene hydroalkoxylation, see: (a) Coulombel, L.; Rajzmann, M.; Pons, J.-M.; Olivero, S.; Duñach, E. *Chem. Eur. J.* **2006**, *12*, 6356–6365. (b) Yang, C.-G.; He, C. *J. Am. Chem. Soc.* **2005**, *127*, 6966–6967. (c) Oe, Y.; Ohta, T.; Ito, Y. *Synlett* **2005**, *1*, 179–181. (d) Qian, H.; Han, X.; Widenhoefer, R. A. *J. Am. Chem. Soc.* **2004**, *126*, 9536–9537.
- (5) For examples of alkyne hydroalkoxylation, see: (a) Wipf, P.; Graham, T. H. *J. Org. Chem.* **2003**, *68*, 8798–8807. (b) Sheng, Y.; Musaev, D. G.; Reddy, K. S.; McDonald, F. E.; Morokuma, K. *J. Am. Chem. Soc.* **2002**, *124*, 4149–4157. (c) Trost, B. M.; Rhee, Y. H. *J. Am. Chem. Soc.* **2002**, *124*, 2528–2533. (d) Kadota, I.; Lutete, L. M.; Shibuya, A.; Yamamoto, Y. *Tetrahedron Lett.* **2001**, *42*, 6207–6210. (e) Pale, P.; Chucho, J. *Eur. J. Org. Chem.* **2000**, 1019–1025. (f) Elgafi, S.; Field, L. D.; Messerle, B. A. *J. Organomet. Chem.* **2000**, *607*, 97–104. (g) McDonald, F. E.; Reddy, K. S.; Díaz, Y. *J. Am. Chem. Soc.* **2000**, *122*, 4304–4309. (h) McDonald, F. E. *Chem. Eur. J.* **1999**, *5*, 3103–3106. (i) Tzalis, D.; Koradin, C.; Knochel, P. *Tetrahedron Lett.* **1999**, *40*, 6193–6195. (j) Cacchi, S. *J. Organomet. Chem.* **1999**, *576*, 42–64. (k) McDonald, F. E.; Connolly, C. B.; Gleason, M. M.; Towne, T. B.; Treiber, K. D. *J. Org. Chem.* **1993**, *58*, 6952–6953.
- (6) For examples of allene hydroalkoxylation, see: (a) Zhang, Z.; Widenhoefer, R. A. *Angew. Chem., Int. Ed.* **2007**, *46*, 283–285. (b) Ma, S. *Chem. Rev.* **2005**, *105*, 2829–2871. (c) Bates, R. W.; Satcharoen, V. *Chem. Soc. Rev.* **2002**, *31*, 12–21. (d) Mukai, C.; Yamashita, H.; Hanaoka, M. *Org. Lett.* **2001**, *3*, 3385–3387.
- (7) Baldwin, J. E. *J. Chem. Soc., Chem. Commun.* **1976**, 734–735.
- (8) McDonald, F. E.; Reddy, K. S.; Díaz, Y. *J. Am. Chem. Soc.* **2000**, *122*, 4304–4309.
- (9) Trost, B. M.; Rhee, Y. H. *J. Am. Chem. Soc.* **1999**, *121*, 11680–11683.
- (10) (a) Compain, P.; Vatile, J.-M.; Goré, J. *Synlett* **1994**, 943–945. (b) Compain, P.; Goré, J.; Vatile, J.-M. *Tetrahedron Lett.* **1995**, *36*, 4059–4062. (c) Compain, P.; Goré, J.; Vatile, J.-M. *Tetrahedron* **1996**, *52*, 10405–10416.
- (11) (a) Qing, F.-L.; Gao, W.-Z.; Ying, J. *J. Org. Chem.* **2000**, *65*, 2003–2006. (b) Qing, F.-L.; Gao, W.-Z. *Tetrahedron Lett.* **2000**, *41*, 7727–7730.
- (12) (a) Utimoto, K.; Miwa, H.; Nozaki, H. *Tetrahedron Lett.* **1981**, *22*, 4277–4278. (b) Utimoto, K. *Pure Appl. Chem.* **1983**, *55*, 1845–1852.
- (13) Schabbert, S.; Schaumann, E. *Eur. J. Org. Chem.* **1998**, 1873–1878.
- (14) (a) Gabriele, B.; Salerno, G. *Chem. Commun.* **1997**, 1083–1084. (b) Gabriele, B.; Salerno, G.; Lauria, E. *J. Org. Chem.* **1999**, *64*, 7687–7692. (c) Gabriele, B.; Salerno, G.; De Pascali, F.; Scianò, G. T.; Costa, M.; Chiusoli, G. P. *Tetrahedron Lett.* **1997**, *38*, 6877–6880.
- (15) (a) Sieller, B.; Bruneau, C.; Dixneuf, P. H. *J. Chem. Soc., Chem. Commun.* **1994**, 493–494. (b) Sieller, B.; Bruneau, C.; Dixneuf, P. H. *Tetrahedron* **1995**, *51*, 13089–13102.
- (16) Villemin, D.; Goussu, D. *Heterocycles* **1989**, *29*, 1255–1261.
- (17) Luo, F.-T.; Schreuder, I.; Wang, R.-T. *J. Org. Chem.* **1992**, *57*, 2213–2215.
- (18) Pale, P.; Chucho, J. *Tetrahedron Lett.* **1987**, *28*, 6447–6448.

- (19) (a) Hong, S.; Marks, T. J. *Acc. Chem. Res.* **2004**, *37*, 673–686. (b) Yu, X.; Marks, T. J. *Organometallics* **2007**, *26*, 365–376. (c) Ryu, J.-S.; Marks, T. J.; McDonald, F. E. *J. Org. Chem.* **2004**, *69*, 1038–1052. (d) Hong, S.; Marks, T. J. *J. Am. Chem. Soc.* **2002**, *124*, 7886–7887. (e) Ryu, J.-S.; Marks, T. J.; McDonald, F. E. *Org. Lett.* **2001**, *3*, 3091–3094. (f) Arredondo, V. M.; Tian, S.; McDonald, F. E.; Marks, T. J. *J. Am. Chem. Soc.* **1999**, *121*, 3633–3639. (g) Arredondo, V. M.; McDonald, F. E.; Marks, T. J. *J. Am. Chem. Soc.* **1998**, *120*, 4871–4872. (h) Li, Y.; Marks, T. J. *J. Am. Chem. Soc.* **1998**, *120*, 1757–1771. (i) Roesky, P. W.; Stern, C. L.; Marks, T. J. *Organometallics* **1997**, *16*, 4705–4711. (j) Li, Y.; Marks, T. J. *J. Am. Chem. Soc.* **1996**, *118*, 9295–9306. (k) Li, Y.; Marks, T. J. *J. Am. Chem. Soc.* **1996**, *118*, 707–708. (l) Giardello, M. A.; Conticello, V. P.; Brard, L.; Gagné, M. R.; Marks, T. J. *J. Am. Chem. Soc.* **1994**, *116*, 10241–10254. (m) Giardello, M. A.; Conticello, V. P.; Brard, L.; Sabat, M.; Rheingold, A. L.; Stern, C. L.; Marks, T. J. *J. Am. Chem. Soc.* **1994**, *116*, 10212–10240. (n) Li, Y.; Fu, P.-F.; Marks, T. J. *Organometallics* **1994**, *13*, 439–440. (o) Gagné, M. R.; Stern, C. L.; Marks, T. J. *J. Am. Chem. Soc.* **1992**, *114*, 275–294.
- (20) (a) Motta, A.; Fragala, I. L.; Marks, T. J. *Organometallics* **2005**, *24*, 4995–5003. (b) Kawaoka, A. M.; Douglass, M. R.; Marks, T. J. *Organometallics* **2003**, *22*, 4630–4632. (c) Douglass, M. R.; Ogasawara, M.; Hong, S.; Metz, M. V.; Marks, T. J. *Organometallics* **2002**, *21*, 283–292. (d) Douglass, M. R.; Stern, C. L.; Marks, T. J. *J. Am. Chem. Soc.* **2001**, *123*, 10221–10238.
- (21) For recent organolanthanide reviews, see: (a) Amin, S. B.; Marks, T. J. *Angew. Chem., Int. Ed.* **2008**, *47*, 2006–2025. (b) Aspinall, H. C. *Chem. Rev.* **2002**, *102*, 1807–1850. (c) Edelmann, F. T.; Freckmann, D. M. M.; Schumann, H. *Chem. Rev.* **2002**, *102*, 1851–1896. (d) Arndt, S.; Okuda, J. *Chem. Rev.* **2002**, *102*, 1953–1976. (e) Molander, G. A.; Romero, A. C. *Chem. Rev.* **2002**, *102*, 2161–2186. (f) Shibasaki, M.; Yoshikawa, N. *Chem. Rev.* **2002**, *102*, 2187–2210. (g) Inanaga, J.; Furuno, H.; Hayano, T. *Chem. Rev.* **2002**, *102*, 2211–2226. (h) Molander, G. A. *Chemtracts: Org. Chem.* **1998**, *18*, 237–263. (i) Edelmann, F. T. *Top. Curr. Chem.* **1996**, *179*, 247–276. (j) Edelmann, F. T. In *Comprehensive Organometallic Chemistry*; Wilkinson, G., Stone, F. G. A., Abel, E. W., Eds.; Pergamon Press: Oxford, 1995; Vol. 4, Chapter 2. (k) Schumann, H.; Meese-Marktscheffel, J. A.; Esser, L. *Chem. Rev.* **1995**, *95*, 865–986. (l) Marks, T. J.; Ernst, R. D. In *Comprehensive Organometallic Chemistry*; Wilkinson, G., Stone, F. G. A., Abel, E. W., Eds.; Pergamon Press: Oxford, 1982; Chapter 21.
- (22) Shen, Q.; Huang, W.; Wang, J.; Zhou, X. *Organometallics* **2008**, *27*, 301–303.
- (23) Zhang, L.; Wang, S.; Sheng, E.; Zhou, S. *Green Chem.* **2005**, *7*, 683–686.

Scheme 1. Proposed Catalytic Cycle and Thermodynamic Considerations for Representative Lanthanide-Mediated Hydroalkoxylation/Cyclizations of C–C Unsaturated Alcohols



Bonding energetic considerations³³ for the unexplored organolanthanide-mediated hydroalkoxylation of alkynyl alcohols predict that the insertion of C–C unsaturation into Ln–O bonds (Scheme 1, step *i*) is significantly more exothermic ($\Delta H \approx -13$ kcal/mol) than for terminal alkenes ($\Delta H \approx +22$ kcal/mol) and that the subsequent Ln–C protonolysis step (Scheme 1, step *ii*) is exothermic for both terminal alkynes ($\Delta H \approx -26$ kcal/mol) and alkenes ($\Delta H \approx -36$ kcal/mol). Thus, the net hydroalkoxylation of both alkenyl and alkynyl alcohols is estimated to be exothermic (Scheme 1); however, the very large Ln–O bond enthalpy^{33a} renders insertive step *i* very, perhaps prohibitively, endothermic for alkenyl alcohols. In a recent communication, we briefly reported using a limited set of substrates and precatalysts, that organolanthanide-catalyzed hydroalkoxylation of alkynyl alcohols can be a viable process with appropriate catalysts and reaction conditions.³² However, these observations raise significant questions about scope and mechanism vis-à-vis more conventional hydroalkoxylation. Herein we report a detailed scope/kinetic/mechanistic study of catalytic alkynyl alcohol hydroalkoxylation. In this full account, reaction scope, stereoselectivity, metal ion effects, and reaction kinetics are examined in detail and compared/contrasted with previously characterized intramolecular hydroamination/- and hydrophosphination/cyclization processes.

Experimental Section

Materials and Methods. All manipulations of air-sensitive materials were carried out with rigorous exclusion of oxygen and moisture in flame- or oven-dried Schlenk-type glassware on a dual-manifold Schlenk line, interfaced to a high-vacuum line (10^{-6} Torr), or in a nitrogen-filled vacuum atmosphere glovebox with a high capacity recirculator (<1 ppm of O_2). Argon (Airgas, prepurified) was purified by passage through a MnO oxygen-removal column and a Davison 4 A molecular sieve column. Pentane was dried using activated alumina columns according to the method described by Grubbs.³⁴ Ether and THF were distilled from sodium benzophenone ketyl. Benzene was dried by vacuum-transfer from Na/K alloy immediately prior to use if employed for catalyst synthesis or catalytic reactions. D_2O (Cambridge Isotope Laboratories; all 99+ atom % D) was used directly as received. Benzene- d_6 (Cambridge Isotope Laboratories; all 99+ atom % D) used for NMR reactions and kinetic measurements was stored in vacuo over Na/K alloy in

resealable bulbs and was vacuum-transferred immediately prior to use. Substrates **1**, **9**, **17**, **21**, and **41** were purchased from Sigma-Aldrich Co, substrate **46** was purchased from TCI, and substrates **3**,³² **5**,³⁵ **7**,³⁶ **13**,³⁷ **19**,³⁸ **27**,³⁹ **29**,⁴⁰ **31**,⁴¹ **33**,^{42,5e} **35**,⁴³ **48**,^{44,45c} **51**,⁴⁵ **55**,⁴³ and **58**^{45a} were prepared as reported in the literature. All liquid substrates were dried twice as solutions in benzene- d_6 over freshly activated Davison 4 A molecular sieves and were degassed by freeze–pump–thaw methods. They were then stored in vacuum-tight storage flasks. Solid substrates were sublimed under high-vacuum and stored in the glovebox before use. The lanthanide complexes $Ln[N(SiMe_3)_2]_3$ ($Ln = La, Nd, Sm, Y,$ and Lu) were prepared according to published procedures.⁴⁶ The 1H NMR integration internal standard Ph_3SiMe was purchased from Strem Inc., sublimed under high vacuum, and stored in the glovebox before use.

Physical and Analytical Measurements. NMR spectra were recorded on a Varian Gemini 300 (300 MHz, 1H ; 75 MHz, ^{13}C), Mercury-400 (FT, 400 MHz, 1H ; 100 MHz, ^{13}C), or Inova-500 (500 MHz, 1H ; 125 MHz, ^{13}C , 76.7 MHz, 2H) instrument. Chemical shifts (δ) for 1H , 2H , and ^{13}C are referenced to internal solvent resonances and reported relative to $SiMe_4$. NMR experiments on air-sensitive samples were conducted in Teflon valve-sealed J. Young tubes. Mass spectra data were obtained on a Varian 1200 Quadrupole mass spectrometer and Micromass Quadro II spectrometer. Elemental analyses were performed by Midwest Micro-labs, Indianapolis, IN.

Synthesis of 1-(2-(Prop-2-ynyl)phenyl)ethanol (37). Dimethyl sulfoxide (DMSO) (1.16 mL, 16.4 mmol) was added over a period of 20 min at -78 °C to a stirring 2 M solution of oxalyl chloride (7.5 mL, 15.1 mmol) dissolved in CH_2Cl_2 (80 mL). After the

- (24) (a) Komeyama, K.; Sasayama, D.; Kawabata, T.; Takehira, K.; Takaki, K. *Chem. Commun.* **2005**, 634–636. (b) Komeyama, K.; Sasayama, D.; Kawabata, T.; Takehira, K.; Takaki, K. *J. Org. Chem.* **2005**, *70*, 10679–10687.
- (25) (a) Komeyama, K.; Kawabata, T.; Takehira, K.; Takaki, K. *J. Org. Chem.* **2005**, *70*, 7260–7266. (b) Nishiura, M.; Hou, Z.; Wakatsuki, Y.; Yamaki, T.; Miyamoto, T. *J. Am. Chem. Soc.* **2003**, *125*, 1184–1185. (c) Nishiura, M.; Hou, Z. *J. Mol. Catal. A* **2004**, *213*, 101–106.
- (26) Li, Q. H.; Wang, S. W.; Zhou, S. L.; Yang, G. S.; Zhu, X. C.; Liu, Y. Y. *J. Org. Chem.* **2007**, *72*, 6763–6767.
- (27) (a) Horino, Y.; Livinghouse, T. *Organometallics* **2004**, *23*, 12–14. (b) Gountchev, T.; Tilley, T. D. *Organometallics* **1999**, *18*, 5661–5667.
- (28) Horino, Y.; Livinghouse, T.; Stan, M. *Synlett* **2004**, 2639–2641.
- (29) (a) Chen, Y. H.; Zhu, Z. Y.; Zhang, J.; Shen, J. Z.; Zhou, X. G. *J. Organomet. Chem.* **2005**, *690*, 3783–3789. (b) Burgstein, M. R.; Berberich, H.; Roesky, P. W. *Chem. Eur. J.* **2001**, *7*, 3078–3085. (c) Berberich, H.; Roesky, P. W. *Angew. Chem., Int. Ed.* **1998**, *37*, 1569–1571.
- (30) Seo, S.; Marks, T. J. *Org. Lett.* **2008**, *10*, 317–319.
- (31) (a) Motta, A.; Fragala, I. L.; Marks, T. J. *Organometallics* **2006**, *25*, 5533–5539. (b) Motta, A.; Lanza, G.; Fragala, I. L.; Marks, T. J. *Organometallics* **2004**, *23*, 4097–4104. (c) Ryu, J.; Li, G. Y.; Marks, T. J. *J. Am. Chem. Soc.* **2003**, *125*, 12584–12605. (d) Kim, Y. K.; Livinghouse, T.; Bercaw, J. E. *Tetrahedron Lett.* **2001**, *42*, 2933–2935.
- (32) Yu, X.; Seo, S.; Marks, T. J. *J. Am. Chem. Soc.* **2007**, *129*, 7244–7245.
- (33) (a) Nolan, S. P.; Stern, D.; Marks, T. J. *J. Am. Chem. Soc.* **1989**, *111*, 7844–7853. (b) McMillen, D. F.; Golden, D. M. *Annu. Rev. Phys. Chem.* **1982**, *33*, 493–532. (c) Benson, S. W. *Thermochemical Kinetics*, 2nd ed.; John Wiley and Sons: New York, 1976; Appendix Tables A10, 11, and 22. (d) Giardello, M. A.; King, W. A.; Nolan, S. P.; Porchia, M.; Sishta, C.; Marks, T. J. In *Energetics of Organometallic Species*; MartinhoSimoes, J. A., Ed.; Kluwer: Amsterdam, 1992; pp 35–54. (e) Gagné, M. R.; Nolan, S. P.; Seyan, A. M.; Stern, D.; Marks, T. J. In *Metal–Metal Bonds and Clusters in Chemistry and Catalysis*; Fackler, J. P., Ed.; Plenum Press: New York, 1990; pp 113–125. (f) Marks, T. J. In *Bonding Energetics in Organometallic Compounds*; Marks, T. J., Ed.; ACS Symposium Series 428; American Chemical Society: Washington, DC, 1990; pp 1–18. (g) Nolan, S. P.; Stern, D.; Hedden, D.; Marks, T. J. In *Bonding Energetics in Organometallic Compounds*; Marks, T. J., Ed.; ACS Symposium Series 428; American Chemical Society: Washington, DC, 1990; pp 159–174.

solution was stirred at $-78\text{ }^{\circ}\text{C}$ for an additional 10 min. (2-(prop-2-ynyl)phenyl)methanol (**19**) (1.0 g, 6.84 mmol) dissolved in CH_2Cl_2 (30 mL) was next added dropwise. The reaction mixture was stirred at $-78\text{ }^{\circ}\text{C}$ for 30 min, and triethylamine (4.8 mL, 34.2 mmol) was then added dropwise at $-78\text{ }^{\circ}\text{C}$. The reaction mixture was stirred for an additional 30 min and then allowed to warm to room temperature. Water (100 mL) and CH_2Cl_2 (100 mL) were next added, and the resulting two layers were separated. The organic layer was washed with 10% aqueous HCl, then washed with brine. The organic layer was next dried over Na_2SO_4 . After filtration, the solvent was removed in vacuo to yield a pale yellow liquid. Without further purification, the crude aldehyde was dissolved in dry ether (50 mL) at $-78\text{ }^{\circ}\text{C}$. A 3.0 M solution of MeMgCl (3.4 mL, 10.3 mmol) was added with stirring to the reaction mixture at $-78\text{ }^{\circ}\text{C}$ over a period of 30 min. The reaction mixture was next warmed to room temperature and stirred for an additional 1 h. The reaction mixture was then quenched with 10% HCl solution (50 mL) and extracted with ether. The combined ether extracts were washed with brine and dried over Na_2SO_4 . After filtration, the solvent was removed in vacuo. Column chromatography on silica gel (hexane/ $\text{EtOAc} = 5:1$) afforded pure alcohol **37** (568 mg; 52% yield); ^1H NMR (500 MHz, CDCl_3): δ 7.55 (d, 7.8 Hz, 1H), 7.44 (d, 7.8 Hz, 1H), 7.35–7.27 (m, 2H), 5.22 (q, 6.8 Hz, 1H), 3.65 (m, 1H), 2.21 (t, 2.9 Hz, 1H), 1.91 (br, 1H), 1.53 (d, 5.9 Hz, 3H); ^{13}C NMR (125 MHz, CDCl_3): δ 143.35, 133.10, 129.41, 128.06, 127.90, 125.68, 82.39, 71.12, 66.67, 24.22, 22.44; Anal. Calcd for $\text{C}_{11}\text{H}_{12}\text{O}$: C, 82.46; H, 7.55. Found: C, 82.60; H, 7.57.

Synthesis of 2-Amino-1-(2-ethynylphenyl)ethanol (39). The reagent 2-ethynylbenzaldehyde (1.94 g, 14.9 mmol) was added to a stirring aqueous 2 M NaHSO_3 solution (20 mL). After the solution was stirred at $0\text{ }^{\circ}\text{C}$ for an additional 10 min, potassium cyanide (3.9 g, 60 mmol) in water (50 mL) was added. After 2 h of stirring, the solution was then extracted with ether ($3 \times 70\text{ mL}$). The extracts were washed twice with aqueous 2 M NaHSO_3 solution, once with water, and dried over Na_2SO_4 . After filtration, the solvent was removed in vacuo to yield a pale yellow solid. This crude cyanohydrin was used without further purification for the next step.

- (34) Pangborn, A. B.; Giardello, M. A.; Grubbs, R. H.; Rosen, R. K.; Timmers, F. J. *Organometallics* **1996**, *15*, 1518–1520.
- (35) (a) Rigby, J. H.; Laxmisha, M. S.; Hudson, A. R.; Heap, C. H.; Heeg, M. J. *J. Org. Chem.* **2004**, *69*, 6751–6760. (b) Magnus, P.; Principe, L. M.; Slater, M. J. *J. Org. Chem.* **1987**, *52*, 1483–1486.
- (36) (a) Chen, Y.; Lee, C. *J. Am. Chem. Soc.* **2006**, *128*, 15598–15599. (b) Ohiai, M.; Nishi, Y.; Mori, T.; Tada, N.; Suefujii, T.; Frohn, H. J. *J. Am. Chem. Soc.* **2005**, *127*, 10460–10461.
- (37) Kamijo, S.; Dudley, G. B. *J. Am. Chem. Soc.* **2006**, *128*, 6499–6507.
- (38) (a) Chang, S.; Lee, M.; Jung, D. Y.; Yoo, E. J.; Cho, S. H.; Han, S. K. *J. Am. Chem. Soc.* **2006**, *128*, 12366–12367. (b) Patil, N. T.; Lutete, L. M.; Wu, H.; Pahadi, N. K.; Gridnev, I. D.; Yamamoto, Y. *J. Org. Chem.* **2006**, *71*, 4270–4279.
- (39) Janza, B.; Studer, A. *Org. Lett.* **2006**, *8*, 1875–1878.
- (40) (a) Kamijo, S.; Dudley, G. B. *Tetrahedron Lett.* **2006**, *47*, 5629–5632. (b) Knoess, H. P.; Furlong, M. T.; Rozema, M. J.; Knochel, P. *J. Org. Chem.* **1991**, *56*, 5974–5978.
- (41) Luo, F. T.; Schreuder, I.; Wang, R. T. *J. Org. Chem.* **1992**, *57*, 2213–2215.
- (42) Trost, B. M.; Pinkerton, A. B. *J. Am. Chem. Soc.* **2002**, *124*, 7376–7389.
- (43) Padwa, A.; Krumpke, K. E.; Weingarten, M. D. *J. Org. Chem.* **1995**, *60*, 5595–5603.
- (44) (a) Rosillo, M.; Dominguez, G.; Casarrubios, L.; Amador, U.; Perez-Castells, J. *J. Org. Chem.* **2004**, *69*, 2084–2093. (b) Bacchi, A.; Costa, M.; Della Ca, N.; Fabbriatore, M.; Fazio, A.; Gabriele, B.; Nasi, C.; Salerno, G. *Eur. J. Org. Chem.* **2004**, 574–585.
- (45) (a) Fischer, D.; Tomeba, H.; Pahadi, N. K.; Patil, N. T.; Yamamoto, Y. *Angew. Chem., Int. Ed.* **2007**, *46*, 4764–4766. (b) Sashida, H.; Ohyanagi, K.; Minoura, M.; Akiba, K. *J. Chem. Soc., Perkin Trans. I* **2002**, 606–612. (c) Villemin, D.; Goussu, D. *Heterocycles* **1989**, *29*, 1255–1261.
- (46) (a) Schuetz, S. A.; Day, V. W.; Sommer, R. D.; Rheingold, A. L.; Belot, J. A. *Inorg. Chem.* **2001**, *40*, 5292–5295. (b) Bradley, D. C.; Ghotra, J. S.; Hart, F. A. *J. Chem. Soc., Dalton Trans.* **1973**, 1021–1023. (c) Alyea, E. C.; Bradley, D. C.; Copperthwaite, R. G. *J. Chem. Soc., Dalton Trans.* **1972**, 1580–1584.

To a stirred suspension of LiAlH_4 (541 mg, 14.3 mmol) in Et_2O at $0\text{ }^{\circ}\text{C}$ under N_2 was slowly added a solution of the above cyanohydrin (1.12 g, 7.1 mmol) in Et_2O . The reaction mixture was allowed to warm to room temperature and stirred under reflux for 2 h. Next, the mixture was diluted with Et_2O and then carefully quenched by sequential additions of water, 15% aqueous NaOH, and water. Stirring at room temperature for a further 30 min yielded a colorless solution with a white precipitate, which was then removed by filtration through a Celite pad. The filtrate was then dried over Na_2SO_4 , filtered, and concentrated under reduced pressure. Column chromatography on silica gel ($\text{CH}_2\text{Cl}_2/\text{MeOH} = 10:1$) afforded pure **39** (681 mg; 28% yield); ^1H NMR (500 MHz, CDCl_3): δ 7.53 (d, 7.8 Hz, 1H), 7.45 (d, 7.8 Hz, 1H), 7.35 (d, 7.8 Hz, 1H), 7.20 (d, 7.8 Hz, 1H), 5.08 (q, 3.9 Hz, 1H), 3.30 (s, 1H), 3.0 (d, 11.7 Hz, 1H), 2.76 (q, 6.8 Hz, 1H), 2.54 (br, 3 H); ^{13}C NMR (125 MHz, CDCl_3): δ 145.46, 133.04, 129.37, 127.26, 125.88, 119.72, 82.39, 81.64, 72.30, 48.35; Anal. Calcd for $\text{C}_{10}\text{H}_{11}\text{NO}$: C, 74.51; H, 6.88; N, 8.69; O, 9.93. Found: C, 74.48; H, 6.99; N, 8.59; O, 9.97.

Typical NMR-Scale Catalytic Reactions. In a glovebox, the homoleptic lanthanide amide $\text{Ln}[\text{N}(\text{SiMe}_3)_2]_3$ (5 μmol) and methyltriphenylsilane (53.2 μmol , internal integration standard) were weighed into a vial, and 500 μL of benzene- d_6 was added by syringe. The solution was mixed to yield a homogeneous, clear solution which was then transferred to a J. Young NMR tube equipped with a Teflon valve. The tube was next closed, removed from the glovebox and attached to the high-vacuum line. The substrate (ca. 1.0 M in benzene- d_6 , 0.10 mL, 20-fold molar excess) was added by syringe to the catalyst solution under an argon stream. The NMR tube was next sealed and frozen at $-78\text{ }^{\circ}\text{C}$ until the time for NMR analysis and then brought to the desired temperature, and the ensuing hydroalkoxylation/cyclization reaction was monitored by ^1H NMR spectroscopy.

Typical Preparative-Scale Catalytic Reactions. Scale-up catalytic reactions were carried out using the following procedure. In a glovebox, the homoleptic lanthanide amide $\text{La}[\text{N}(\text{SiMe}_3)_2]_3$ (31 mg, 50 μmol) was weighed into a vial, and 500 μL of benzene- d_6 was added by syringe. The reagents were mixed to yield a homogeneous, clear solution and transferred to a storage tube equipped with a Teflon valve and a magnetic stir bar. The tube was then closed, removed from the glovebox, and attached to the high-vacuum line. The substrate (ca. 1.0 M in benzene- d_6 , 1 mL, 20-fold molar excess) was added by syringe to the catalyst solution under an argon stream. The mixture was then freeze–pump–thaw degassed and warmed to room temperature. The resulting solution was stirred with heating to $60\text{ }^{\circ}\text{C}$ for 5 h. At completion of the reaction, this reaction mixture was filtered through a small plug of silica gel to remove the catalyst. This crude product was then purified by flash column chromatography or Kugelrohr distillation.

Synthesis of 3-Methylene-2-oxa-spiro[4.5]decane (8). ^1H NMR (500 MHz, C_6D_6): δ 4.55 (s, 1H), 3.93 (s, 1H), 3.55 (s, 2H), 2.07 (s, 2H), 1.12–1.09 (m, 10H); ^{13}C NMR (125 MHz, C_6D_6): δ 163.05, 80.10, 70.54, 42.05, 41.10, 34.20, 26.05, 23.43. HRMS-ESI(m/z): $[(\text{M} + \text{H})^+]$ calcd for $\text{C}_{10}\text{H}_{17}\text{O}$, 153.1279; found, 153.1276.

Synthesis of 5,5-Dimethyl-2-methylene-tetrahydro-2H-pyran (12). ^1H NMR (500 MHz, C_6D_6): δ 4.61 (s, 1H), 4.10 (s, 1H), 3.32 (s, 2H), 2.05 (t, 6.8 Hz, 2H), 1.15 (t, 5.9 Hz, 2H), 0.70 (s, 6H); ^{13}C NMR (125 MHz, C_6D_6): δ 159.47, 90.95, 78.58, 34.57, 29.57, 25.92, 24.85. HRMS-ESI(m/z): $[(\text{M} + \text{H})^+]$ calcd for $\text{C}_8\text{H}_{15}\text{O}$, 127.1123; found, 127.1119.

Synthesis of 4,4-Dimethyl-2-methylene-tetrahydro-2H-pyran (14). ^1H NMR (500 MHz, C_6D_6): δ 4.66 (s, 1H), 4.06 (s, 1H), 3.67 (t, 5.9 Hz, 2H), 1.81 (s, 2H), 1.09 (t, 5.9 Hz, 2H), 0.74 (s, 6H); ^{13}C NMR (125 MHz, C_6D_6): δ 159.01, 92.19, 65.13, 43.14, 37.95, 32.11, 27.83. HRMS-ESI(m/z): $[(\text{M} + \text{H})^+]$ calcd for $\text{C}_8\text{H}_{15}\text{O}$, 127.1123; found, 127.1118.

Synthesis of 3,3-Dimethyl-2-methylene-tetrahydro-2H-pyran (16). ^1H NMR (500 MHz, C_6D_6): δ 4.62 (s, 1H), 4.25 (s, 1H), 3.61 (t, 5.4 Hz, 2H), 1.39–1.34 (m, 2H), 1.22 (t, 5.9 Hz, 2H), 1.05 (s,

6H); ^{13}C NMR (125 MHz, C_6D_6): δ 169.21, 90.68, 70.61, 37.80, 34.44, 27.60, 22.81. HRMS-ESI(m/z): $[(\text{M} + \text{H})^+]$ calcd for $\text{C}_8\text{H}_{15}\text{O}$, 127.1123; found, 127.1120.

Synthesis of 2-Methyl-5-methylene-tetrahydrofuran (26). ^1H NMR (500 MHz, C_6D_6): δ 4.51(s, 1H), 3.96(m, 1H), 3.87(s, 1H), 2.22–2.17(m, 2H), 1.47–1.43(m, 2H), 1.00(d, 6.8 Hz, 3H); ^{13}C NMR (125 MHz, C_6D_6): δ 163.01, 78.83, 78.08, 32.35, 29.63, 20.54. HRMS-ESI(m/z): $[(\text{M} + \text{H})^+]$ calcd for $\text{C}_6\text{H}_{11}\text{O}$, 99.0810; found, 99.0807.

Synthesis of 2-Methylene-6-phenyl-tetrahydro-2H-pyran (30). ^1H NMR (500 MHz, C_6D_6): δ 7.29 (d, 7.8 Hz, 2H), 7.14 (t, 7.8 Hz, 2H), 7.07 (d, 7.8 Hz, 1H), 4.66 (s, 1H), 4.47–4.44 (dd, 12.7 Hz, 2.9 Hz, 1H), 2.03–1.98 (m, 2H), 1.51–1.35 (m, 4H); ^{13}C NMR (125 MHz, C_6D_6): δ 160.66, 142.99, 128.36, 127.50, 125.95, 92.14, 81.02, 33.50, 28.97, 23.35. HRMS-ESI(m/z): $[(\text{M} + \text{H})^+]$ calcd for $\text{C}_{12}\text{H}_{15}\text{O}$, 175.1123; found, 175.1112.

Synthesis of 1-Methyl-3-methylene-1,3-dihydroisobenzofuran (36). ^1H NMR (500 MHz, C_6D_6): δ 7.20 (t, 4.4 Hz, 1H), 6.97 (m, 2H), 6.68 (t, 4.4 Hz, 1H), 5.18 (q, 5.9 Hz, 1H), 4.72 (s, 1H), 4.54 (s, 1H), 1.17 (d, 6.8 Hz, 3H); ^{13}C NMR (125 MHz, C_6D_6): δ 161.37, 145.03, 134.04, 128.83, 128.21, 121.07, 120.69, 80.75, 77.94, 21.26. HRMS-ESI(m/z): $[(\text{M} + \text{H})^+]$ calcd for $\text{C}_{10}\text{H}_{11}\text{O}$, 147.0810; found, 147.0805.

Synthesis of 1-Methyl-3-methyleneisochroman (38). ^1H NMR (500 MHz, C_6D_6): δ 7.04–6.98 (m, 2H), 6.84–6.80 (m, 2H), 4.65 (q, 4.9 Hz, 1H), 4.55 (s, 1H), 4.04 (s, 1H), 3.21 (s, 2H), 1.36 (d, 5.9 Hz, 3H); ^{13}C NMR (125 MHz, C_6D_6): δ 156.33, 138.93, 134.05, 128.21, 126.64, 126.44, 123.37, 85.32, 72.20, 33.65, 18.96. HRMS-ESI(m/z): $[(\text{M} + \text{H})^+]$ calcd for $\text{C}_{11}\text{H}_{13}\text{O}$, 161.0966; found, 161.0960.

Synthesis of (3-Methylene-1,3-dihydroisobenzofuran-1-yl)methanamine (40). ^1H NMR (500 MHz, C_6D_6): δ 7.20 (t, 5.9 Hz, 1H), 6.96 (t, 3.9 Hz, 2H), 6.75 (t, 4.9 Hz, 1H), 5.04 (t, 4.4 Hz, 1H), 4.70 (s, 1H), 4.53 (s, 1H), 2.76–2.73 (m, 1H), 2.64–2.60 (m, 1H), 0.58 (br, 2H); ^{13}C NMR (125 MHz, C_6D_6): δ 161.68, 141.70, 134.98, 128.82, 128.21, 121.48, 120.67, 86.32, 77.98, 46.89. HRMS-ESI(m/z): $[(\text{M} + \text{H})^+]$ calcd for $\text{C}_{10}\text{H}_{12}\text{NO}$, 162.0919; found, 162.0913.

Synthesis of (E)-((Dihydrofuran-2(3H)-ylidene)methyl)trimethylsilane (42). ^1H NMR (500 MHz, C_6D_6): δ 4.78 (s, 1H), 3.58 (t, 6.8 Hz, 2H), 2.13 (t, 7.8 Hz, 2H), 1.33 (m, 2H), 0.15 (s, 9H); ^{13}C NMR (125 MHz, C_6D_6): δ 168.13, 86.69, 69.19, 28.93, 25.35, 2.52. HRMS-ESI(m/z): $[(\text{M} + \text{H})^+]$ calcd for $\text{C}_8\text{H}_{17}\text{OSi}$, 157.1049; found, 157.1041.

Synthesis of (E)-(Isobenzofuran-1(3H)-ylidenemethyl)trimethylsilane (49). ^1H NMR (500 MHz, C_6D_6): δ 7.65 (d, 7.8 Hz, 1H), 7.43 (d, 7.8 Hz, 1H), 7.08 (t, 7.8 Hz, 1H), 6.87 (t, 7.8 Hz, 1H), 5.05 (s, 2H), 4.77 (s, 1H), 0.07 (s, 9H); ^{13}C NMR (125 MHz, C_6D_6): δ 169.61, 145.87, 136.39, 135.58, 129.54, 128.09, 127.83, 100.17, 75.91, –3.33. HRMS-ESI(m/z): $[(\text{M} + \text{H})^+]$ calcd for $\text{C}_{12}\text{H}_{17}\text{OSi}$, 205.1049; found, 205.1042.

Synthesis of Trimethyl(2-((trimethylsilyl)ethynyl)benzoyloxy)silane (50). ^1H NMR (500 MHz, C_6D_6): δ 7.65 (d, 7.8 Hz, 1H), 7.43 (d, 7.8 Hz, 1H), 7.08 (t, 7.8 Hz, 1H), 6.87 (t, 7.8 Hz, 1H), 5.03 (s, 2H), 0.22 (s, 9H), 0.11 (s, 9H); ^{13}C NMR (125 MHz, C_6D_6): δ 143.80, 132.10, 128.95, 126.78, 126.63, 103.43, 99.35, 62.98, –0.04, –0.55. Anal. Calcd for $\text{C}_{15}\text{H}_{24}\text{OSi}_2$: C, 65.15; H, 8.75. Found: C, 65.37; H, 8.92.

Synthesis of (E)-Trimethyl(3-methylisobenzofuran-1(3H)-ylidene)methyl)silane (56). ^1H NMR (500 MHz, C_6D_6): δ 7.77 (d, 6.8 Hz, 1H), 7.01 (m, 2H), 6.68 (t, 4.9 Hz, 1H), 5.22 (s, 1H), 5.14 (q, 5.9 Hz, 1H), 1.17 (d, 6.8 Hz, 3H), 0.30 (s, 9H); ^{13}C NMR (125 MHz, C_6D_6): δ 165.58, 147.70, 134.05, 133.74, 128.20, 123.27, 121.44, 90.03, 79.44, 21.25, 2.54. HRMS-ESI(m/z): $[(\text{M} + \text{H})^+]$ calcd for $\text{C}_{13}\text{H}_{19}\text{OSi}$, 219.1205; found, 219.1200.

Synthesis of Trimethyl(1-(2-((trimethylsilyl)ethynyl)phenyl)ethoxy)silane (57). ^1H NMR (500 MHz, C_6D_6): δ 7.70 (d, 7.8 Hz, 1H), 7.42 (d, 7.8 Hz, 1H), 7.06 (t, 7.8 Hz, 1H), 6.83 (t, 7.8 Hz,

1H), 5.66 (q, 5.9 Hz, 1H), 1.56 (d, 5.9 Hz, 3H), 0.23 (s, 9H), 0.11 (s, 9H); ^{13}C NMR (125 MHz, C_6D_6): δ 149.56, 132.08, 129.24, 126.79, 125.70, 120.08, 103.89, 99.11, 68.75, 26.17, –0.04, –0.15. Anal. Calcd for $\text{C}_{16}\text{H}_{26}\text{OSi}_2$: C, 66.14; H, 9.02. Found: C, 66.18; H, 9.14.

Synthesis of (E)-1-Benzylidene-3-methyl-1,3-dihydroisobenzofuran (59). ^1H NMR (500 MHz, C_6D_6): δ 7.47 (d, 8.2 Hz, 1H), 7.36 (d, 7.0 Hz, 2H), 7.12 (t, 7.0 Hz, 2H), 7.03 (d, 8.2 Hz, 1H), 6.88 (t, 7.0 Hz, 1H), 6.72 (t, 7.0 Hz, 1H), 6.67 (d, 7.0 Hz, 1H), 6.50 (s, 1H), 5.21 (m, 1H), 1.21 (d, 7.0 Hz, 3H); ^{13}C NMR (125 MHz, C_6D_6): δ 156.13, 146.78, 136.56, 132.80, 129.84, 128.96, 126.47, 125.53, 123.20, 121.09, 120.07, 100.63, 79.70, 21.41. HRMS-ESI(m/z): $[(\text{M} + \text{H})^+]$ calcd for $\text{C}_{16}\text{H}_{15}\text{O}$, 223.1123; found, 223.1122.

Kinetic Studies of Hydroalkoxylation/Cyclization. In a typical experiment, an NMR sample was prepared as described above (see Typical NMR-Scale Catalytic Reactions) but maintained at -78°C until kinetic measurements were begun. The sample tube was inserted into the probe of the INOVA-400 spectrometer which had been previously set to the desired temperature ($T \pm 0.1^\circ\text{C}$; checked with a methanol or ethylene glycol temperature standard). A single acquisition ($nt = 1$) with a 45° pulse was used during data acquisition to avoid saturation. The data were processed with the SigmaPlot 2000 program.⁴⁷ The product concentration was measured from the area of the olefinic peak cis to oxygen, A_s , standardized to A_i , the methyl peak area of the Ph_3SiMe internal standard. The turnover frequency, N_t (h^{-1}), was calculated from the least-squares determined slope (m) according to eq 8 where $[\text{catalyst}]_0$ is the initial concentration of the precatalyst.

$$[\text{product}] = mt \quad (7)$$

$$N_t(\text{h}^{-1}) = \frac{60 \text{ min}}{\text{h}} \times \frac{m}{[\text{catalyst}]_0} \quad (8)$$

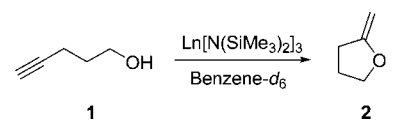
Results

The principal goal of this contribution is to explore the scope and selectivity of the lanthanide-mediated intramolecular hydroalkoxylation/cyclization of alkynyl alcohols, in search of general, highly stereoselective catalytic pathways for heterocycle construction. First, metal effects on the course and rates of the catalytic intramolecular hydroalkoxylation/cyclizations of various alkynyl alcohols are described. Second, the effects of varying substrate substituents on the intramolecular hydroalkoxylation/cyclizations are explored, including the rates and stereochemistry of transformations involving terminal primary alkynyl alcohols, terminal secondary alkynyl alcohols, and internal alkynyl alcohols. Finally, reaction kinetics and mechanistic pathways are discussed, including rate laws, activation parameters, kinetic isotope effects, and their mechanistic implications.

Metal Ion Effects on Catalytic Alkynyl Alcohol Hydroalkoxylation/Cyclization. In the case of aminoalkene hydroamination/cyclization, both increasing the Ln^{3+} ionic radius and opening the metal coordination sphere by *ansa*-fusion of the ancillary ligands⁴⁸ increases the turnover frequencies (N_t 's), presumably reflecting the significant steric demands in the olefinic insertive transition state. This mechanistic scenario is supported by DFT level quantum chemical calculations.^{31b} Catalyst structural effects qualitatively similar to those in aminoalkene hydroamination/cyclization are also operative in the present case. Thus, for the representative cyclization $1 \rightarrow 2$, Table 1 shows that N_t increases substantially with increasing metal ionic radius.⁴⁹

(47) SigmaPlot 2000 version 6.0., SPSS Inc, Chicago, IL, 2000.

(48) Jeske, G.; Schock, L. E.; Mauermann, H.; Swepston, P. N.; Schumann, H.; Marks, T. J. *J. Am. Chem. Soc.* **1985**, *107*, 8103–8110.

Table 1. Effect of Varying Lanthanide Metal Center Ionic Radius on Turnover Frequencies in Catalytic Intramolecular Hydroalkoxylation/Cyclization


entry	Ln	ionic radius (Å)	N_t (h ⁻¹ , °C) ^a
1	La	1.160	4.3(60)
2	Nd	1.109	4.2(60)
3	Sm	1.079	2.1(60)
4	Y	1.019	0.13(60)
5	Lu	0.977	0.2(60)

^a Turnover frequencies measured in benzene-*d*₆ with 5 mol % precatalyst.

Therefore, alkynyl alcohol hydroalkoxylation/cyclization experiences an appreciable acceleration in rate when larger ionic radius Ln³⁺ catalysts are employed, and kinetic data argue that the turnover-limiting step is C≡C insertion into the Ln–O bond (Scheme 1, step *i*; see below).

Scope of Catalytic Intramolecular Hydroalkoxylation/Cyclization of Terminal Alkynyl Alcohols. Homoleptic Ln[N(SiMe₃)₂]₃ lanthanide amido complexes serve as effective precatalysts for the clean and, in most cases, quantitative intramolecular hydroalkoxylation/cyclization of terminal alkynyl alcohols to yield the corresponding furan, pyran, benzofuran, and isochroman heterocycles as summarized in Tables 2 and 3, where N_t is the catalytic turnover frequency at the temperature indicated.⁵⁰ In general, the catalytic hydroalkoxylation/cyclization reactions of terminal alkynyl alcohols proceed to completion at 25–130 °C under inert atmosphere, at 5 mol % catalyst loading in 1 h to 3 days. In the present study, homoleptic lanthanide amides, Ln[N(SiMe₃)₂]₃, are found by ¹H NMR spectroscopy to undergo essentially instantaneous Ln–N bond protonolysis by the C–C unsaturated alcohols at room temperature to yield the corresponding alkoxides and free HN(SiMe₃)₂. At 60 °C, substrate **1** undergoes conversion to cyclic methyltetrahydrofuran **2** within 5 h with 5 mol % La[N(SiMe₃)₂]₃ as the precatalyst. The reaction progress is conveniently monitored from intensity changes in the substrate olefinic resonances by ¹H NMR spectroscopy, using evolved HN(SiMe₃)₂ or added Ph₃SiMe as internal NMR standards (Figure 1). Turnover frequencies were determined in benzene-*d*₆ from the slope of the kinetic plots of substrate: catalyst ratio vs time. The final furan, pyran, benzofuran, and isochroman products were vacuum transferred with any other volatiles, and were characterized by ¹H, ¹³C NMR spectroscopy, and high-resolution MS or elemental analysis (see Experimental Section for details).

The anaerobic cyclization of a diverse series of alkynyl alcohols, mediated by the homoleptic La[N(SiMe₃)₂]₃ lanthanide amido precatalysts, proceeds with near-quantitative conversions and reasonably rapid turnover frequencies at 25–120 °C (Tables 2 and 3). The reaction scope was designed to probe a variety of structural effects on this catalytic transformation, including

(49) Representative eight-coordinate effective ionic radii: La(III), 1.160 Å; Nd(III), 1.109 Å; Sm(III), 1.079 Å; Y(III), 1.019 Å; Yb(III), 0.985 Å; Lu(III), 0.977 Å. See Shannon, R. D. *Acta Crystallogr., Sect. A* **1976**, *A32*, 751–767.

(50) (a) The phenolic substrate 2-(prop-2-ynyl)phenol^{50b} was tested under the same reaction conditions. However, the reaction progressed only 6% to completion at 120 °C over 2 days. (b) Zhang, Q.; Takacs, J. M. *Org. Lett.* **2008**, *10*, 545–548.

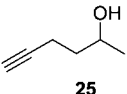
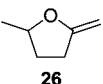
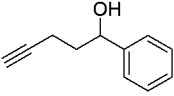
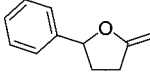
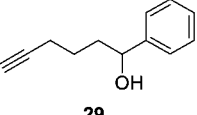
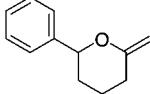
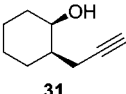
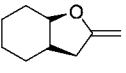
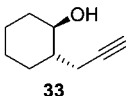
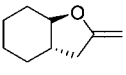
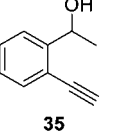
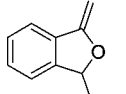
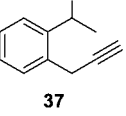
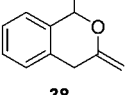
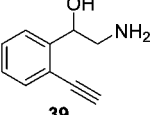
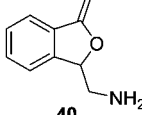
Table 2. Catalytic Lanthanide-Mediated Intramolecular Hydroalkoxylation/Cyclization of Primary Terminal Alkynyl Alcohols

Entry	Substrate	Product ^a	N_t (h ⁻¹ , °C) ^b
1	1	2	0.5(40) 1.4(50) 4.3(60) 8.6(70) 23.3(80)
2	3	2, 4a-c	4.1(60)
3	5	6	18.0(60)
4	7	8	38.5(60)
5	9	10	0.11(120)
6	11	12	0.36(120)
7	13	14	0.32(120)
8	15	16	0.34(120)
9	17	18	9.8(60)
10	19	20	5.4(120)
11	21	22	8.7(25) 230.1(60)
12	23	24	4.7(120)

^a Yields ≥ 95% by ¹H NMR spectroscopy and GC/MS. ^b Turnover frequencies measured in benzene-*d*₆ with 5 mol % precatalyst.

five- and six-membered ring formation using a variety of primary and secondary alcohols. It is found that furans (Table 2, entries 1, 3, 4, and 11; Table 3, entries 1, 2, 4, and 5), pyrans (Table 2, entries 5–8; Table 3, entry 3), benzofurans (Table 2, entry 9; Table 3, entries 6 and 8), and isochromans (Table 2, entry 10; Table 3, entry 7) are cleanly formed via 5- and 6-*exo* cyclization, respectively, and that there is no evidence of alternative 6- or 7-*endo* cyclizations. As observed for the organolanthanide-mediated hydroamination/cyclization of aminoalkenes,^{19c,e,l,m} aminoalkynes,^{19h,j,k} and aminoallenes,^{19f,g} the ring-size dependence of cyclization rates (N_t) for the present primary and secondary alkynyl alcohols is 5 > 6, consistent with a classical, stereoelectronically controlled cyclization

Table 3. Catalytic Lanthanide-Mediated Intramolecular Hydroalkoxylation/Cyclization of Secondary Terminal Alkynyl Alcohols

Entry	Substrate	Product ^a	N_t (h^{-1} , $^{\circ}\text{C}$) ^b
1			0.91(60)
2			2.8(60)
3			0.14(120)
4			10.2(60)
5			1.5(60)
6			52.8(25)
7			1.4(60)
8			9.4(60)

^a Yields $\geq 95\%$ by ^1H NMR spectroscopy and GC/MS. ^b Turnover frequencies measured in benzene- d_6 with 5 mol % precatalyst.

process (Table 2, entry 1 vs 5, entry 9 vs 10; Table 3, entry 2 vs 3, entry 6 vs 7).⁵¹ Geminal dialkyl substitution of the carbon backbone (the Thorpe–Ingold effect,⁵² Table 2, entries 3–4) increases the N_t 's by ~ 5 – $9\times$ in the case of five-membered ring formation, as also observed in organolanthanide-mediated aminoalkene hydroamination.^{19c,e} Thus, the $5 \rightarrow 6$ and $7 \rightarrow 8$ transformations are significantly more rapid than $1 \rightarrow 2$ ($N_t = 18.0, 38.5$ vs 4.3 h^{-1} at 60 $^{\circ}\text{C}$). Furthermore, the six-membered ring cyclization of primary alkynyl alcohols (Table 2, entries 6–8) also exhibits a Thorpe–Ingold effect ($N_t = 0.36, 0.34, 0.32$ vs 0.11 h^{-1} at 120 $^{\circ}\text{C}$) but somewhat slower cyclization rates versus the five-membered ring cyclizations. A similar explanation invoking some combination of the Thorpe–Ingold

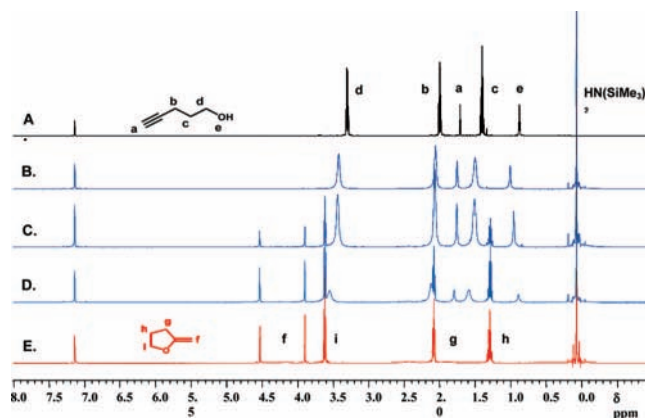


Figure 1. ^1H NMR monitoring (500 MHz) of the cyclization $1 \rightarrow 2$ mediated by a $\text{La}[\text{N}(\text{SiMe}_3)_2]_3$ precatalyst in benzene- d_6 at 60 $^{\circ}\text{C}$ (A) pent-4-yn-1-ol (**1**), (B) 0, (C) 1.0, (D) 3.0, and (E) 5.0 h.

effect and electronic factors is also plausible for arene-substituted substrates (Table 2, entries 9–10). Thus, for five-membered ring formation, the $17 \rightarrow 18$ transformation is significantly more rapid than $1 \rightarrow 2$ ($N_t = 9.8$ vs 4.3 h^{-1} at 60 $^{\circ}\text{C}$). In the case of six-membered ring formation, the $19 \rightarrow 20$ transformation is significantly more rapid than $9 \rightarrow 10$ ($N_t = 5.4$ vs 1.1 h^{-1} at 120 $^{\circ}\text{C}$).

The secondary alkynyl alcohol cases raise more complex questions about those structural effects governing cyclization rates. For linear secondary alkynyl alcohols, the cyclization rate is significantly diminished. For five-membered ring formation, the $25 \rightarrow 26$ and $27 \rightarrow 28$ transformations are significantly slower than $1 \rightarrow 2$ ($N_t = 0.91, 2.8$ vs 4.3 h^{-1} at 60 $^{\circ}\text{C}$). Moreover, the six-membered ring formation process reveals that there are minimal differences between primary and secondary alkynyl alcohols ($29 \rightarrow 30$ vs $9 \rightarrow 10$; $N_t = 0.14$ vs 0.11 h^{-1} at 120 $^{\circ}\text{C}$, respectively). However, aromatic substrate functionalization enhances cyclization rates; thus, the $35 \rightarrow 36$ transformation is significantly more rapid than $17 \rightarrow 18$ ($N_t = 52.8$ h^{-1} at 25 $^{\circ}\text{C}$ vs 9.8 h^{-1} at 60 $^{\circ}\text{C}$), and the $37 \rightarrow 38$ transformation is significantly more rapid than $19 \rightarrow 20$ ($N_t = 1.4$ h^{-1} at 60 $^{\circ}\text{C}$ vs 5.4 h^{-1} at 120 $^{\circ}\text{C}$). An interesting observation concerning this transformation is that there is marked selectivity for oxygen over nitrogen hydrofunctionalization (Table 2, entry 12 and Table 3, entry 8).

Stereoselectivity Issues for Internal Alkynyl Alcohols in Hydroalkoxylation/Cyclization. The intramolecular hydroalkoxylation/cyclization of internal alkynyl alcohols mediated by the homoleptic $\text{Ln}[\text{N}(\text{SiMe}_3)_2]_3$ lanthanide amido precatalysts proceeds effectively, selectively, and with high conversions to yield the corresponding furans and benzofurans, as shown in Table 4, where N_t is the catalytic turnover frequency at the temperature indicated. In general, the catalytic hydroalkoxylation/cyclization reactions of the internal alkynyl alcohols examined proceed to completion at 60 – 130 $^{\circ}\text{C}$ under inert atmosphere, at 5 mol % catalyst loading in 1 h to 3 days. Reaction progress is conveniently monitored from intensity changes in substrate olefinic resonances by ^1H NMR spectroscopy, using evolved $\text{HN}(\text{SiMe}_3)_2$ and added Ph_3SiMe as convenient internal NMR standards as discussed above. Turnover frequencies were calculated in benzene- d_6 from the slope of the kinetic plots of substrate: catalyst ratio vs time. The final products were vacuum transferred with other volatiles and characterized by ^1H , ^{13}C NMR spectroscopy, NOESY, and high-resolution MS or elemental analysis (see Experimental Section for data). Accord-

(51) (a) Carey, F. A.; Sundberg, R. J. *Advanced Organic Chemistry*, 4th ed.; Kluwer Academic/ Plenum Publishers: New York, 2000; Part A, Chapter 3.9. (b) Illuminati, G.; Mandoline, L. *Acc. Chem. Res.* **1981**, *14*, 95–102.

(52) (a) Eliel, E. L.; Wilen, S. H.; Mander, L. N. *Stereochemistry of Organic Compounds*; Wiley-Interscience: New York, 1994; pp 682–684. (b) Kirby, A. J. *Adv. Phys. Org. Chem.* **1980**, *17*, 183–278.

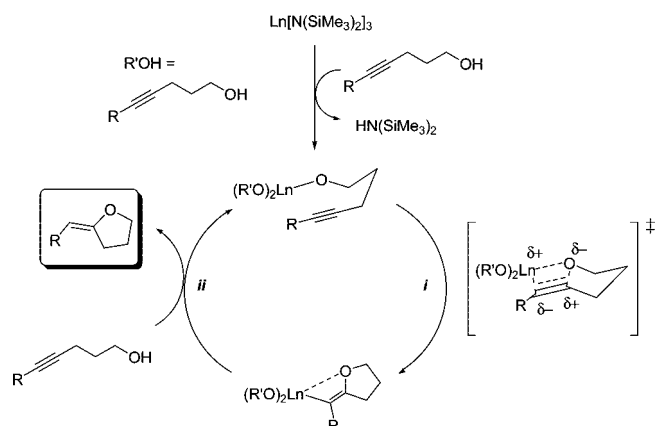
Table 4. Lanthanide-Mediated Catalytic Intramolecular Hydroalkoxylation/Cyclization of Internal Alkynyl Alcohols

Entry	Substrate	Product ^a	N_t (h ⁻¹ , °C) ^b
1		 	0.9(130)
2			~0.02(120)
3			1.34(120)
4		 	9.3(90) 24.4(120)
5			6.1(90)
6			6.4(90)
7		 	32.8(60)
8			1.52(70)

^a Yields $\geq 95\%$ by ¹H NMR spectroscopy and GC/MS. ^b Turnover frequencies measured in benzene-*d*₆ with 5 mol % precatalyst.

ing to a plausible mechanistic pathway for internal alkynyl alcohol hydroalkoxylation/cyclization (Scheme 2), the turnover-limiting step is likely to be insertion step *i*, according to Scheme 1 and other mechanistic data (see more below). Here, the stereochemistry of the principal product is expected to be the *E*-conformer. Indeed, the actual stereochemistry is confirmed to be the *E*-conformer by NOESY experiments.

The scope of the present organolanthanide-mediated hydroalkoxylation/cyclization of internal alkynyl alcohols is summarized in Table 4. Under identical reaction conditions, the cyclization rates of internal alkynyl alcohols (Table 4) are significantly slower than those of the corresponding terminal alkynyl alcohols (Tables 2 and 3). For the linear internal alkynyl alcohols, the cyclization rates are also diminished in comparison to the terminal alkynyl alcohols. The relative rates of linear internal alkynyl alcohol conversion as a function of substituent R are $-\text{H} > -\text{Ph} > -\text{SiMe}_3 > -\text{Me}$ (Table 2, entry 1; Table

Scheme 2. Proposed Catalytic Cycle for Lanthanide-Mediated Hydroalkoxylation/Cyclization of Internal Alkynyl Alcohols

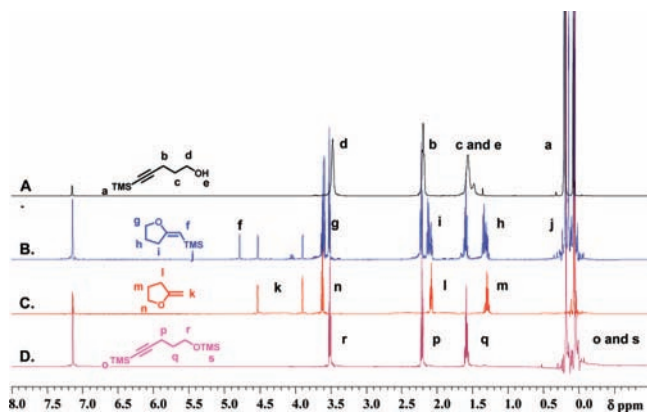
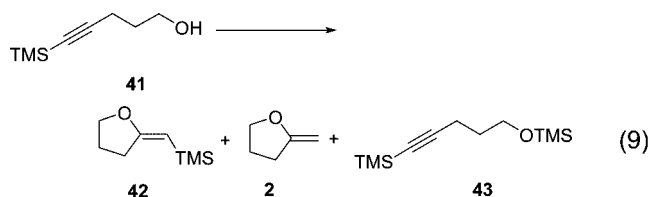


Figure 2. ^1H NMR spectra (500 MHz) of 5 mol % $\text{La}[\text{N}(\text{SiMe}_3)_2]_3$ precatalyst in benzene- d_6 at 130 °C in the presence of a 20-fold excess of 5-(trimethylsilyl)pent-4-yn-1-ol (**41**) (A) $t = 0$ h, (B) after completion of reaction, (C) after cyclization completion of pent-4-yn-1-ol (**1**), and (D) trimethyl(5-(trimethylsilyl)pent-4-yn-1-yl)silane (**43**).

4, entries 1–3), while the relative rates of hydroalkoxylation/cyclization for aromatic internal alkynyl alcohols as a function of substituent R are $-\text{H} > -\text{SiMe}_3 > -\text{Ph}$ (Table 2, entry 9; Table 4, entries 4–5 and Table 3, entry 6; Table 4, entries 6–7). Aromatic substrate substitution increases cyclization rates compared to the linear internal alkynyl alcohols, with relative rates following the same general trend as in the terminal alkynyl alcohols. Thus, for **48** \rightarrow **49** and **55** \rightarrow **56**, the transformation is significantly more rapid than for **41** \rightarrow **42** ($N_t = 9.3 \text{ h}^{-1}$ at 90 °C, 32.8 h^{-1} at 60 °C vs 0.9 h^{-1} at 130 °C) with $\text{R} = -\text{SiMe}_3$, and the **51** \rightarrow **52** and **58** \rightarrow **59** transformations are faster than for **46** \rightarrow **47** ($N_t = 6.1 \text{ h}^{-1}$ at 90 °C, 1.52 h^{-1} at 70 °C vs 1.34 h^{-1} at 120 °C).

An interesting observation in the hydroalkoxylation/cyclization of the SiMe_3 -terminated alkynyl alcohols is the variety of reaction products detected in the ^1H NMR spectroscopy, as shown in Figure 2. Through careful ^1H , ^{13}C NMR spectroscopic analysis, GC-MS, and high-resolution MS techniques, we surmise that this reaction mixture consists of three discrete products. For the substrate 5-(trimethylsilyl)pent-4-yn-1-ol (**41**), the products are the desired product **42**, SiMe_3 -deprotected product **2**, and SiMe_3 -protected starting material **43** (eq 9).



Kinetic and Mechanistic Studies of Alkynyl Alcohol Hydroalkoxylation/Cyclization. Quantitative kinetic studies of the representative cyclization **1** \rightarrow **2** were carried out with 1.1–10.0 mol % of precatalyst in benzene- d_6 at 60 °C by ^1H NMR spectroscopic monitoring. The increase of one olefinic resonance (either that at $\delta \approx 3.8$ or at 4.5 ppm) was monitored by ^1H NMR spectroscopy and integrated versus $\text{HN}(\text{SiMe}_3)_2$ ($\delta \approx 0.2$ ppm), which is stoichiometrically generated upon substrate addition (Figure 1) and/or versus methyltriphenylsilane (Ph_3SiMe), the internal NMR integration standard. The methyl signal of methyltriphenylsilane (δ 0.7 ppm) can be readily distinguished from the substrate **1** and product **2** resonances, and from various catalyst signals at 500 MHz. These cyclizations

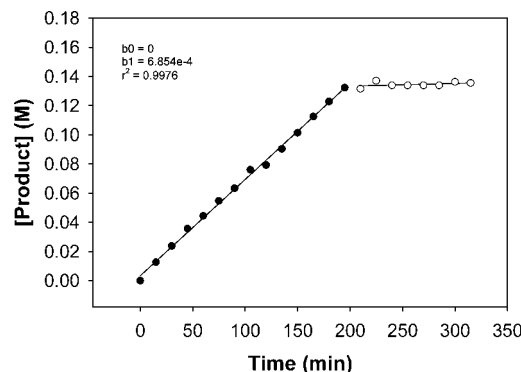


Figure 3. Concentration of product **2** (methylene-tetrahydrofuran) as a function of time for the hydroalkoxylation/cyclization of pent-4-yn-1-ol (**1**) using 5 mol % $\text{La}[\text{N}(\text{SiMe}_3)_2]_3$ as the precatalyst in benzene- d_6 at 60 °C. The circles indicate completion of the conversion.

were performed with a 10–90-fold molar excess of substrate over catalyst, and in all cases substrate was completely consumed.

The linear increase of olefin concentration with conversion (Figure 3) suggests zero-order dependence on substrate concentration. When the initial concentration of alkynyl alcohol is held constant and the concentration of precatalyst varied over 10-fold range, a plot of reaction rate vs precatalyst concentration (Figure 4A) and a plot of $\ln(\text{rate})$ vs $\ln[\text{catalyst}]$ (van't Hoff plot, slope = reaction order, Figure 4B) indicate the reaction to be the first-order in [catalyst]. Overall, the empirical rate law can be expressed as in eq 10, and is identical to that determined for organolanthanide-catalyzed hydroamination/cyclization.¹⁹ Variable-temperature kinetic studies were conducted by in situ

$$\text{rate} = k[\text{substrate}]^0[\text{catalyst}]^1 \quad (10)$$

^1H NMR spectroscopy for transformation **1** \rightarrow **2** mediated by $\text{La}[\text{N}(\text{SiMe}_3)_2]_3$. Data are shown in Figure 5A normalized to the internal standard. The cyclization rate for **1** \rightarrow **2** mediated by $\text{La}[\text{N}(\text{SiMe}_3)_2]_3$ is independent of substrate concentration over a 40 °C temperature range (40–80 °C), suggesting zero-order dependence on substrate concentration. Standard Eyring (Figure 5B) and Arrhenius (Figure 5C) kinetic analyses⁵³ yield activation parameters $\Delta H^\ddagger = 20.2(1.0) \text{ kcal/mol}$, $\Delta S^\ddagger = -11.8(0.3) \text{ e.u.}$, and $E_a = 20.9(0.3) \text{ kcal/mol}$.⁵⁴

An $-\text{OH}$ vs $-\text{OD}$ isotopic labeling study (Table 2, entry 2), assayed by ^1H and ^2H NMR spectroscopy of substrate and product (Figure 6), reveals the interesting observation that substrate **3** yields not only methylene-tetrahydrofuran **4b**, but also isotopomers **2**, **4a**, and **4c** (eq 11). A plausible mechanism which accounts for this product distribution is presented in the Discussion section below. The measured turnover frequency for substrate **3** conversion is only slightly smaller than that of substrate **1**. However, these turnover frequencies do not yield tractable kinetic isotope effect (KIE) data because of the complexity of equilibria operative and the product distribution. In order to obtain KIE data, an internal alkynyl alcohol substrate was examined. Thus, substrate **53** was selected and the hydroalkoxylation/cyclization kinetics of substrate **53** were measured (eq 12), yielding a KIE of $k_{\text{H}}/k_{\text{D}} = 0.95(0.03)$.

Discussion

Scope of Catalytic Intramolecular Hydroalkoxylation/Cycliza-

(53) (a) Robinson, P. J. *J. Chem. Educ.* **1978**, *55*, 509–510. (b) Benson, S. W. *Thermochemical Kinetics*, 2nd ed.; Wiley: New York, 1986; p 810.

(54) Parameters in parentheses represent 3σ values derived from the least-squares fit.

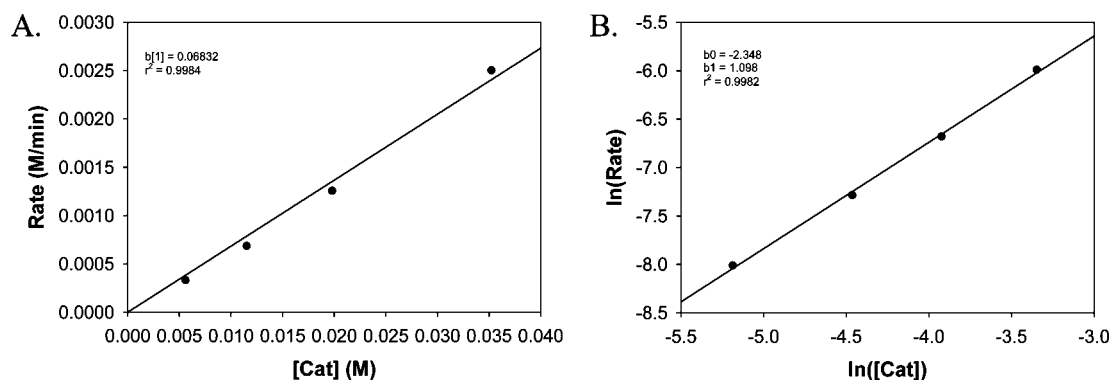
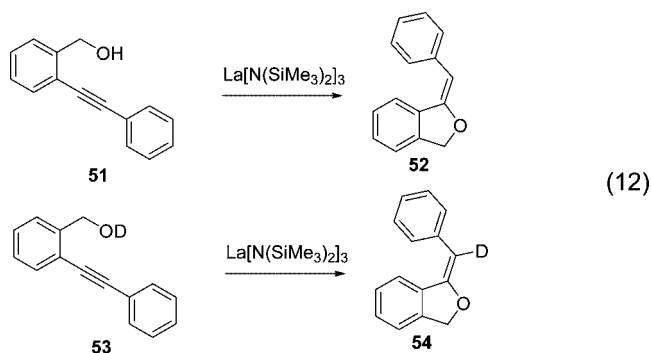
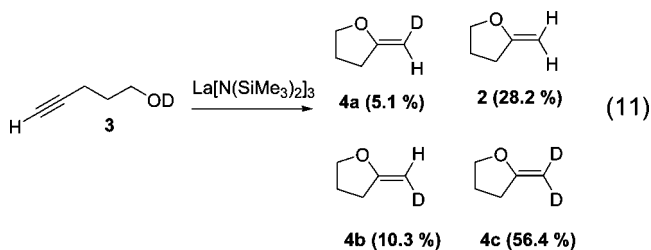
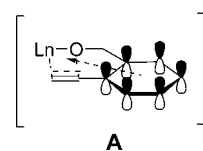


Figure 4. (A) Determination of reaction order in lanthanide concentration for the hydroalkoxylation/cyclization of pent-4-yn-1-ol (**1**) to methylenetetrahydrofuran (**2**) using the $\text{La}[\text{N}(\text{SiMe}_3)_2]_3$ precatalyst in benzene- d_6 at 60 °C. (B) van't Hoff plot of the hydroalkoxylation/cyclization of pent-4-yn-1-ol (**1**) using $\text{La}[\text{N}(\text{SiMe}_3)_2]_3$ as the precatalyst in benzene- d_6 at 60 °C. The lines are least-squares fits to the data points.

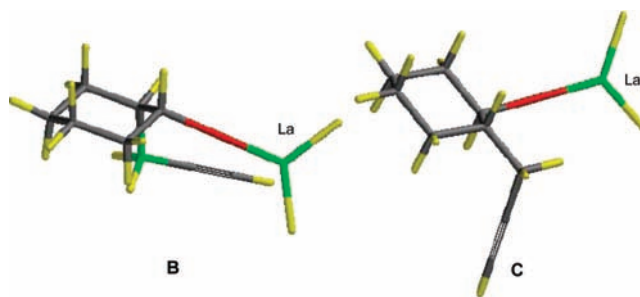


tion of Terminal Alkynyl Alcohols. A central goal of this research was to explore the scope of homoleptic $\text{Ln}[\text{N}(\text{SiMe}_3)_2]_3$ lanthanide amido precatalyst-mediated intramolecular hydroalkoxylation/cyclization of terminal alkynyl alcohols. The results in Tables 2 and 3 indicate that $\text{Ln}[\text{N}(\text{SiMe}_3)_2]_3$ complexes are competent precatalysts for the formation of diverse five- and six-membered heterocycles having a wide variety of alkyl and aryl substituents. In the hydroalkoxylation/cyclization of both primary and secondary alkynyl alcohols, there is a difference in cyclization rate between linear and aromatic alkynyl alcohols. In general, the cyclization rates of the arene-functionalized alkynyl alcohols are more rapid than those of linear alkynyl alcohols. This may reflect configurations in which the arene-functionalized alkynyl alcohols have accessible, more preorganized structures than the linear alkynyl alcohols, involving interaction of the electrophilic lanthanide center with the electron-rich arene π system (A).⁵⁵ Comparison of the primary and secondary alkynyl alcohol cyclization rates indicates that differences in cyclization rates derive from an interplay of complex factors. Thus, the cyclization rates of linear primary alkynyl alcohols are greater than those of linear secondary alkynyl alcohols, while the cyclization rates of arene-functionalized alkynyl alcohols exhibit the opposite trend. This suggests that the interplay of several factors including sterics, electronics

(internal alkynes would be more electron-rich), and metal complexation govern the cyclization rate.



Several substrates having clearly preorganized structures and constrained close approach distances between the alcohol and alkyne functionalities reveal an interesting trend in cyclization rates (Table 2, entry 11; Table 3, entries 4–5). This trend is particularly evident in the hydroalkoxylation/cyclization of substrates **21**, **31**, and **33**. Substrates **31** and **33** have similar chemical structures, differing only in stereochemistry, *syn* and *anti*, respectively. However, cyclization rates differ by a factor of 10 \times . This trend can be understood from the differences in the accessibility/energetics of the respective transition states (compare structures **B** and **C** from Spartan 2002).



Another instructive observation in this work is that these homoleptic $\text{Ln}[\text{N}(\text{SiMe}_3)_2]_3$ lanthanide amido precatalysts exhibit pronounced selectivity in discriminating between C–O and C–N bond formation (Table 2, entry 12 and Table 3, entry 8). Thus, if substrates **23** and **39** were to first undergo C–N bond formation, products **61** and **63** would be obtained and with minimal olefinic resonance intensities expected in the ^1H NMR spectra (eq 13). However, monitoring the reaction progress

(55) For Ln^{3+} -arene complexes, see: (a) Bochkarev, M. N. *Chem. Rev.* **2002**, *102*, 2089–2117. (b) Liang, H.; Shen, Q.; Guan, J.; Lin, Y. *J. Organomet. Chem.* **1994**, *474*, 113–116. (c) Deacon, G. B. *Aust. J. Chem.* **1990**, *43*, 1245–1257. (d) Fan, B.; Shen, Q.; Lin, Y. *J. Organomet. Chem.* **1989**, *376*, 61–66. (e) Fan, B.; Shen, Q.; Lin, Y. *J. Organomet. Chem.* **1989**, *377*, 51–58. (f) Cotton, A.; Schwotzer, W. *Organometallics* **1987**, *6*, 1275–1279. (g) Cotton, A.; Schwotzer, W. *J. Am. Chem. Soc.* **1986**, *108*, 4657–4568.

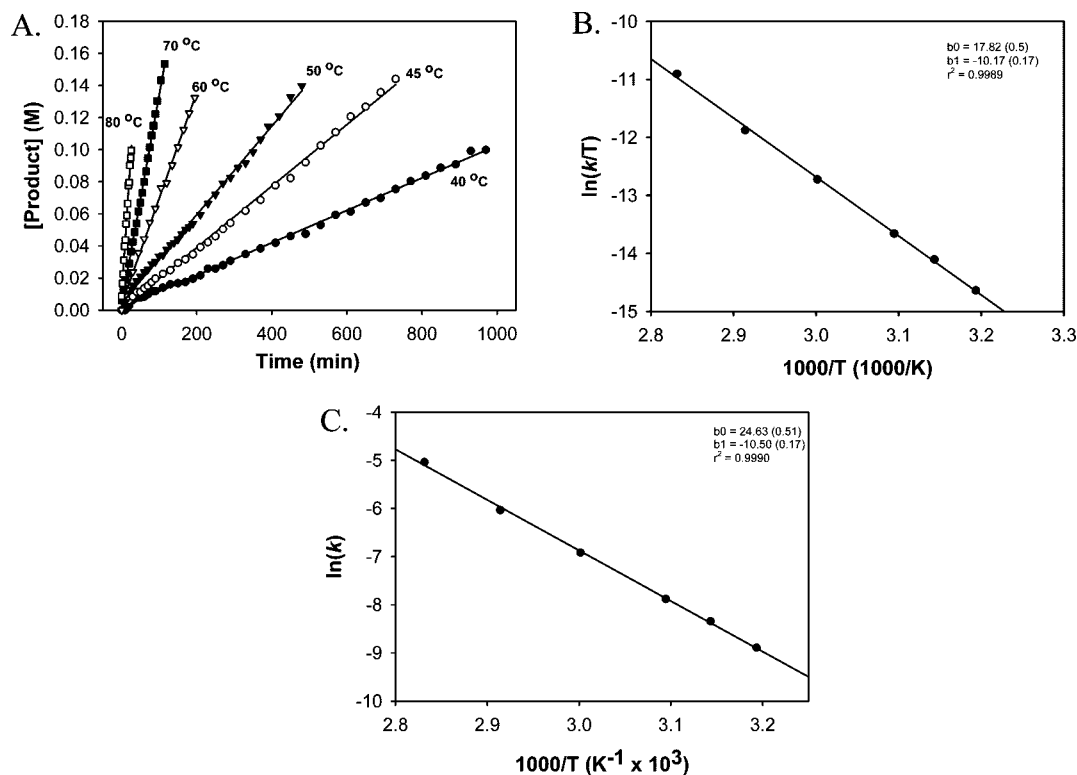


Figure 5. (A) Concentration of product **2** (methylene tetrahydrofuran) as a function of time and temperature for the hydroalkoxylation/cyclization of pent-4-yn-1-ol (**1**) using 5 mol % $\text{La}[\text{N}(\text{SiMe}_3)_2]_3$ as the precatalyst in benzene- d_6 at various temperatures. (B) Eyring plot for the intramolecular hydroalkoxylation/cyclization of **1** using $\text{La}[\text{N}(\text{SiMe}_3)_2]_3$ as the precatalyst in benzene- d_6 . The line represents the least-squares fit to the data points. (C) Arrhenius plot for the intramolecular hydroalkoxylation/cyclization of **1** using $\text{La}[\text{N}(\text{SiMe}_3)_2]_3$ as the precatalyst in benzene- d_6 . The line represents the least-squares fit to the data points.

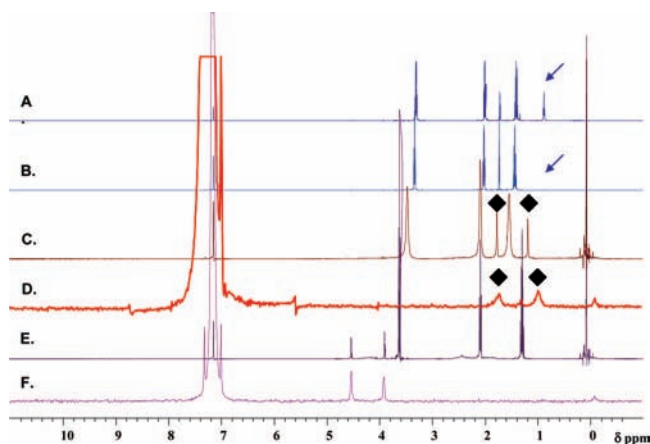
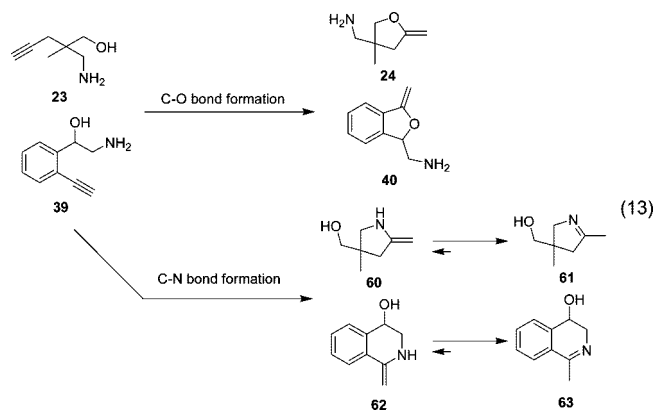


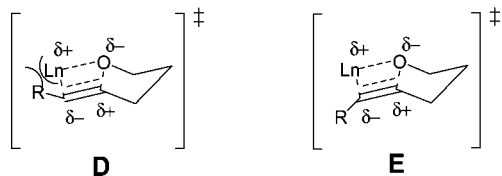
Figure 6. (A) ^1H NMR spectrum (500 MHz) of pent-4-yn-1-ol (**1**) in benzene- d_6 , (B) ^1H NMR spectrum (500 MHz) of pent-4-yn-1-ol-d (**3**) in benzene- d_6 , (C) ^1H NMR spectrum (500 MHz) of pent-4-yn-1-ol-d (**3**) with 5 mol % $\text{La}[\text{N}(\text{SiMe}_3)_2]_3$ precatalyst in benzene- d_6 , (D) ^2H NMR spectrum (77 MHz) of pent-4-yn-1-ol-d (**3**) with 5 mol % $\text{La}[\text{N}(\text{SiMe}_3)_2]_3$ precatalyst in benzene- d_6 , (E) ^1H NMR spectrum (500 MHz) of product (**4a–c** and **2**) with 5 mol % $\text{La}[\text{N}(\text{SiMe}_3)_2]_3$ precatalyst in benzene- d_6 , and (F) ^2H NMR spectrum (77 MHz) of product (**4a–c** and **2**) with 5 mol % $\text{La}[\text{N}(\text{SiMe}_3)_2]_3$ precatalyst in benzene- d_6 . The arrows indicate the resonance of the alcohol (OH) proton, and the diamonds indicate the resonances of the alkyne and alcohol (OH) protons.

reveals olefinic resonances at δ 4.45 and 3.83 ppm for substrate **23** and 4.70 and 4.53 ppm for substrate **39** and the emergence of other features assignable to products **24** and **40** (see Experimental Section for complete characterization data). Therefore, C–O bond formation proceeds selectively with complete (>99%) exclusion of C–N bond formation for this particular catalyst and substrates.

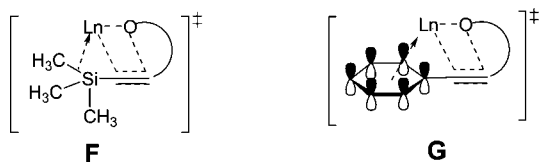


Stereoselectivity in Internal Alkynyl Alcohol Hydroalkoxylation/Cyclization.

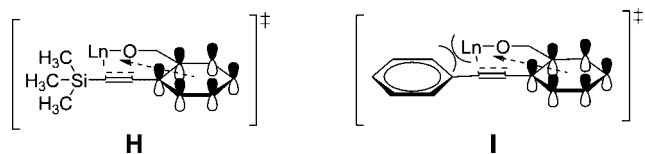
The present lanthanide-mediated hydroalkoxylation/cyclizations of internal alkynyl alcohols proceed with excellent stereoselectivity, and are completely *E*-selective. This high *E*-selectivity can be rationalized in terms of a transition state in which the R substituent occupies the less sterically hindered positions in a chairlike cyclic transition state, similar to those proposed/computed for analogous hydroamination/cyclizations^{19,31} (Scheme 2; **D** versus **E**). Some explanation of R substituent effects on the cyclization reaction kinetics is also possible. Among the principal factors, the interplay of nonbonded repulsions and electronic contributions doubtless govern the hydroalkoxylation/cyclization kinetics. The fact that the cyclization rates of the terminal alkynyl alcohols are invariably greater than those of the internal alkynyl alcohols under identical reaction conditions, as well as that rates increase with increasing Ln^{3+} ionic radius, argues that nonbonded repulsions dominate in the first stages of the cyclization process.



However, the interplay of steric and electronic factors is rather complex in several cases as suggested by the relative rates for $-\text{SiMe}_3$ and $-\text{Ph}$ functionalized substrates. Here, trends are different for linear and aromatic internal alkynyl alcohols. In the linear internal alkynyl alcohol cases, the cyclizations of Ph-substituted internal alkynyl alcohols are more rapid than those of SiMe_3 -substituted internal alkynyl alcohols. This trend may be rationalized by the following explanation. Although the SiMe_3 group exhibits activating effects well-known in organosilicon chemistry,⁵⁶ i.e., β -Si–C bond interactions stabilize electrophilic lanthanide centers (e.g., **F**),^{21k} as suggested by *ab initio* calculations,⁵⁷ arenes have similar activating effects in which the electrophilic lanthanide center interacts with adjacent arene π systems (e.g., **G**),^{55,58} and, additionally, π – π interactions may occur between proximate Ph substituents. Therefore, Ph-

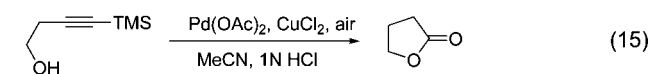
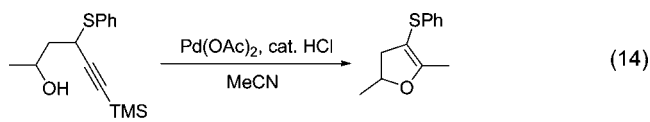


substituted internal alkynyl alcohols may provide the structural rigidity necessary for preorganization-derived rate enhancement. For the aromatic internal alkynyl alcohol systems, the cyclization rates of SiMe_3 -substituted internal alkynyl alcohols are significantly greater than those of the Ph-substituted internal alkynyl alcohols. This trend may be rationalized by a combination of factors, such as steric hindrance, preorganized chemical structure, and transition state electronic demands. In this system class, every substrate has a similar structural backbone, as in substrates **17** and **35**. As noted above, this backbone potentially facilitates preorganized structures and electrophilic Ln^{3+} center–arene π system interactions (**H** and **I**). However, substrates **51** and **58** may also incur nonbonded repulsions between the ligand-bearing Ln^{3+} center and the Ph group (e.g., transition state **I**) resulting in diminished rates.



The loss of terminal alkynyl- SiMe_3 groups during catalytic hydroalkoxylation turnover has been observed by other researchers (e.g., eqs 14 and 15).^{10,13} In both cases, the HCl used in the reaction mixture may play a role in the $-\text{SiMe}_3$ group cleavage. The mechanism of the present cyclization is clearly different because no obvious protic acid is present. From

monitoring the reaction progress by NMR spectroscopy as a



function of time, products **2**, **42**, and **43** (eq 9) are found to appear simultaneously. We tentatively propose the reaction pathway shown in Scheme 3. In the simplest scenario, the first generated catalytic species **A** undergoes cross metathesis with other alcohols to afford complex **B** via two similar routes. Eisen's group has reported similar types of cross metathesis processes for organoaluminum complexes.⁵⁹ Complex **B** can revert to **A** or be transformed to catalytic species **C**. Catalytically active complexes **A** and **C** then generate products **42** and **2**, respectively. Product **43** is generated from the cross metathesis. Under the present conditions, the processes yielding products **2** and **42** are found to have experimentally indistinguishable turnover frequencies: $N_t = 0.9 \text{ h}^{-1}$ at $130 \text{ }^\circ\text{C}$ for **42**; 1.0 h^{-1} at $130 \text{ }^\circ\text{C}$ for **2**.

Kinetics and Mechanism of Alkynyl Alcohol Hydroalkoxylation/Cyclization. The kinetic results for the $1 \rightarrow 2$ transformation catalyzed by $\text{La}[\text{N}(\text{TMS})_2]_3$ indicate zero-order rate dependence on substrate concentration (Figure 3) and first-order dependence on catalyst concentration (Figure 4), similar to the scenario for lanthanocene-mediated intramolecular aminoalkene, aminoalkyne, and aminoallene hydroamination/cyclization and hydrophosphination.^{19,20,31} This result argues that the turnover-limiting step in the present case involves intramolecular $\text{C}\equiv\text{C}$ insertion into the $\text{Ln}-\text{O}$ bond (Scheme 1, step *i*), followed by rapid protonolysis of the resulting $\text{Ln}-\text{C}$ bond (Scheme 1, step *ii*). This cycle would then be followed by transalcoholysis/ligand substitution to introduce another substrate molecule in the Ln^{3+} coordination sphere. These kinetic results also argue that the active catalyst is not in rapid pre-equilibrium with a more associated $[\text{Ln}(\text{OR})_3]_n$ ⁶⁰ species.

An $-\text{OH}$ vs $-\text{OD}$ labeling study (Table 4, entry 6) assayed by ^1H and ^2H NMR spectroscopy yields a kinetic isotope effect (KIE) of $k_{\text{H}}/k_{\text{D}} = 0.95(0.03)$, suggesting a nonprimary isotopic effect and consistent with the alkyne insertion being the turnover-limiting step in the catalytic cycle. However, another labeling study (Table 2, entry2) while not providing straightforward KIE data, yields new insight into details of this hydroalkoxylation/cyclization process. Although *syn*- $\text{Ln}-\text{O}$ addition to substrate **3** would be expected based on the reaction pathway shown in Scheme 1, both *syn*- and *anti*-addition products and other products (**2**, **4a–c**) are detected (eq 11). This observation is supported by ^1H and ^2H NMR spectroscopy (Figure 6). Note that substrate **3** is isotopomerically stable in

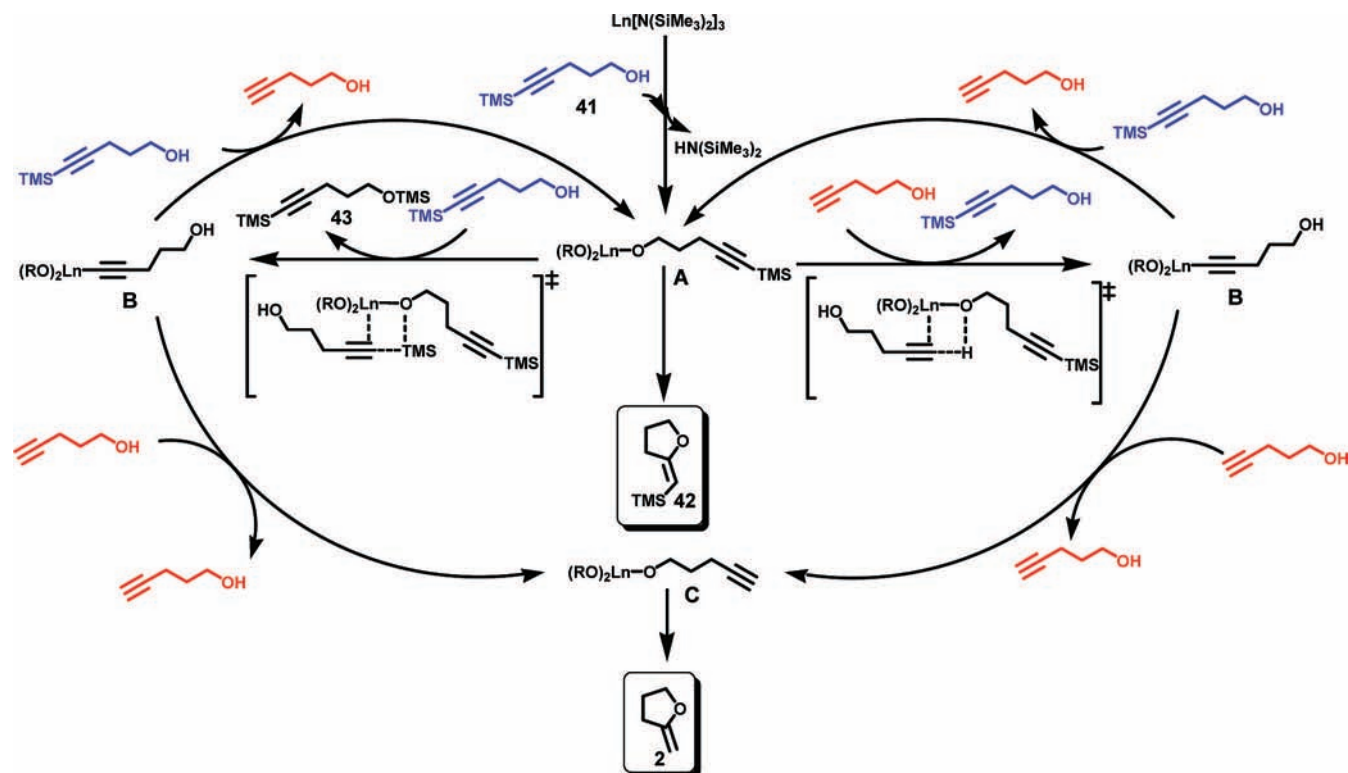
(58) For η^5 -benzylidene organolanthanide structures, see: (a) Evans, W. J.; Ulbarri, T. A.; Ziller, J. W. *J. Am. Chem. Soc.* **1990**, *112*, 219–223. (b) Mintz, E. A.; Moloy, K. G.; Marks, T. J.; Day, V. W. *J. Am. Chem. Soc.* **1982**, *104*, 4692–4695.

(59) (a) Wang, J.; Gurevich, Y.; Botoshansky, M.; Eisen, M. S. *Organometallics* **2008**, *27*, 4494–4504. (b) Wang, J.; Gurevich, Y.; Botoshansky, M.; Eisen, M. S. *J. Am. Chem. Soc.* **2006**, *128*, 9350–9351.

(60) (a) Mehrotra, R. C.; Singh, A.; Tripathi, U. M. *Chem. Rev.* **1991**, *91*, 1287–1303. (b) Sheng, H.; Xu, F.; Yao, Y.; Zhang, Y.; Shen, Q. *Inorg. Chem.* **2007**, *46*, 7722–7724.

(56) (a) Bassindale, A. R.; Taylor, P. G. In *The Chemistry of Organic Silicon Compounds*; Patai, S., Rappaport, Z., Eds.; Wiley: Chichester, UK, 1989; Chapter 14. (b) Fleming, I. In *Comprehensive Organic Chemistry*; Jones, N. D., Ed.; Pergamon Press: Oxford, UK, 1979; Chapter 13.

(57) Koga, N.; Morokuma, K. *J. Am. Chem. Soc.* **1988**, *110*, 108–112.

Scheme 3. Proposed Catalytic Cycle for Lanthanide-Mediated Hydroalkoxylation/Cyclization of SiMe₃-Alkynyl Alcohols**Table 5.** Activation Parameter Comparison for Intramolecular Hydroamination/Cyclization and Hydroalkoxylation/Cyclization Processes

Entry	Substrate	Product	ΔH^\ddagger Kcal/mol	ΔS^\ddagger eu	E_a Kcal/mol
1. ^a			17.7 (2.1)	-24.7 (5)	18.5 (2.0)
2. ^b			16.9 (1.3)	-16.5 (4)	17.6 (1.4)
3. ^c			12.7 (1.4)	-27.0 (5)	13.4 (1.5)
4. ^d			10.7 (8)	-27.4 (6)	11.3 (2.0)
5. ^e			12.3 (1.6)	-25.9(5.2)	13.0(1.4)
6. ^f			20.2 (1.0)	-11.8 (0.3)	20.9 (0.3)

^a Determined using Me₂SiCp''₂SmCH(SiMe₃)₂ as the precatalyst in *o*-xylene-*d*₁₀.^{19c} ^b Determined using Cp'₂LaCH(SiMe₃)₂ as the precatalyst in toluene-*d*₈.^{19g} ^c Determined using Cp'₂LaCH(SiMe₃)₂ as the precatalyst in toluene-*d*₈.¹⁹ⁿ ^d Determined using Cp'₂SmCH(SiMe₃)₂ as the precatalyst in toluene-*d*₈.^{19j} ^e Determined using Cp'₂SmCH(SiMe₃)₂ as the precatalyst in benzene-*d*₆.^{20d} ^f Determined using La[N(SiMe₃)₂]₃ as the precatalyst in benzene-*d*₆.

the absence of the lanthanide precatalyst (Figure 6A and B); however, when the lanthanide precatalyst is added to the substrate **3** solution, equilibration between species **A** and **C** of Scheme 4 is observed (Figure 6C and D). As a control, we

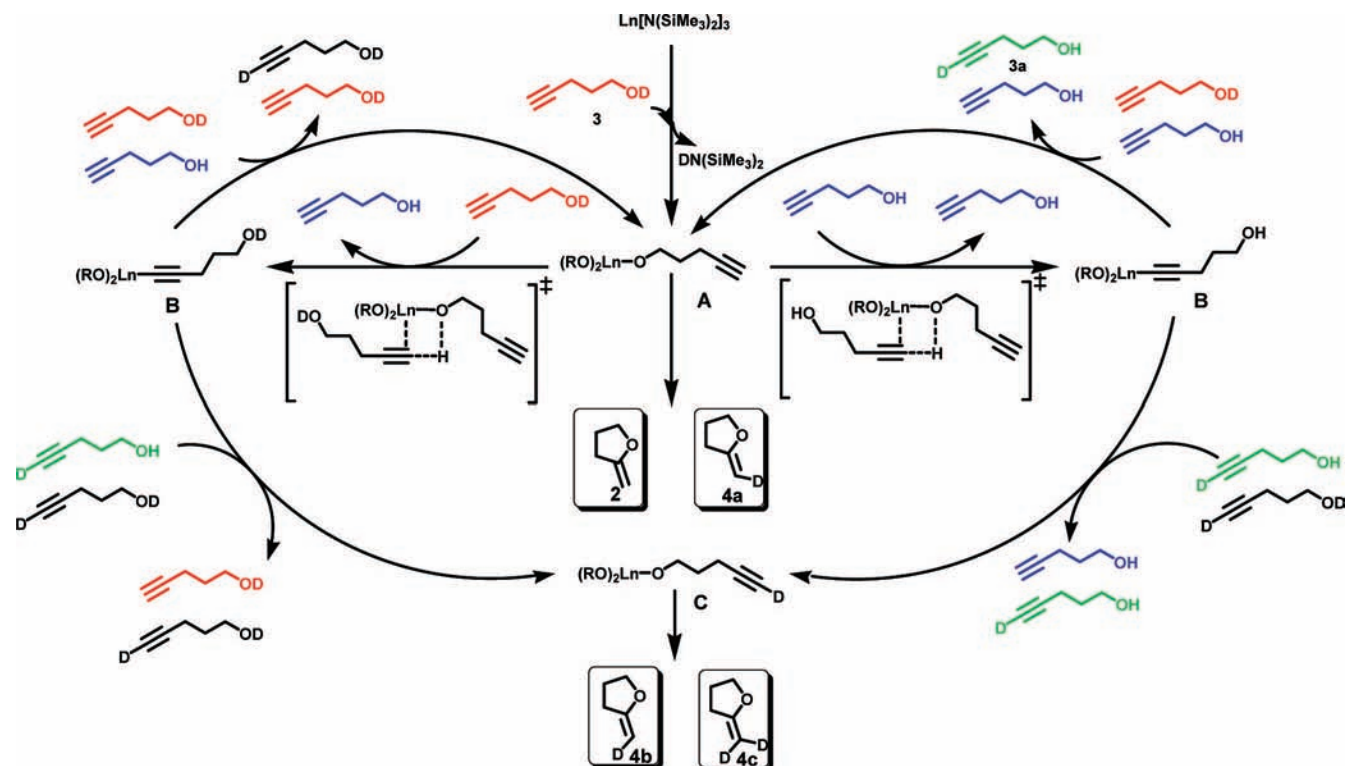
synthesized substrate **3a**⁶¹ and tested its hydroalkoxylation using the same reaction conditions. From this experiment, we find the same product mixture as from the hydroalkoxylation of substrate **3**.

In principal, substrate **3** should afford four compounds (**4a–c** and **2**) according to the proposed reaction pathways shown in Scheme 4. In the ¹H and ²H NMR spectroscopy of the hydroalkoxylation products derived from substrate **3**, NMR resonances not observed in the ¹H NMR spectroscopy of the hydroalkoxylation product of substrate **1** are observed (Figures 7A and B). To validate the assignments, we undertook the synthesis of authentic samples of compounds **2**, **4a**, and **4b** (see Supporting Information). Although these authentic samples contain isomerization impurities, they do not interfere with the ¹H NMR spectroscopic assignments. Figure 7C shows the ¹H NMR spectra of a mixture of authentic samples of **2**, **4a**, and **4b** and the very clear similarity to the spectrum in Figure 7B. On the basis of these experiments, we can assign each alkene peak and find the ratio of each product from integrating the ¹H NMR spectrum, as shown in eq 11. The reaction sequences that afford these products is conceptually similar to that of Scheme 3. Here the first generated catalytically active species **A** undergoes cross metathesis with other alcohols to produce species **B**. **B** can revert to species **A**, when can also form species **C**. Catalytically active species **A** and **C** then generate products **2**, **4a** and **4b**, **4c**, respectively.

The present activation parameters for transformation **1** → **2** can be compared to the corresponding parameters for the hydroamination/cyclization of aminoalkenes, aminoalkynes, and aminoallenes, as well as the hydrophosphination/cyclization of a phosphinoalkene (Table 5). In the present study, hydroalkoxy-

(61) (a) Grant, B.; Djerassi, C. *J. Org. Chem.* **1974**, *39*, 968–970. (b) Thomas, A. F. *Deuterium Labeling in Organic Chemistry*; Meredith Corp.: New York, 1971.

Scheme 4. Proposed Catalytic Cycle for Lanthanide-Mediated Hydroalkoxylation/Cyclization of Deuterated Alkynyl Alcohols



lation/cyclization of an alkynyl alcohol proceeds with the largest ΔH^\ddagger value and the smallest magnitude of ΔS^\ddagger for this series of transformations (Table 5). That the alkynyl alcohol cyclization exhibits greatest enthalpic barrier and the smallest magnitude of ΔS^\ddagger (less negative) implies a rather organized, polar transition state characteristic of many d^0, f^n -centered transformations,¹⁹ and together with the large E_a^\ddagger value doubtless reflects the very large Ln–O bond enthalpy. Overall, the present results obtained from the kinetic studies (rate law, activation parameters) and from structural factors affecting cyclization rates (metal ion size, product ring size, substrate substituent effects) support a

hydroalkoxylation/cyclization mechanistic scenario (Scheme 1)³² roughly analogous to those established for hydroamination/cyclization¹⁹ and hydrophosphination/cyclization,²⁰ but with certain distinctive differences.

Conclusions. Intramolecular hydroalkoxylation/cyclization processes of alkynyl alcohol substrates mediated by homoleptic $\text{Ln}[\text{N}(\text{SiMe}_3)_2]_3$ lanthanide amido precatalysts exhibit a broad reaction scope in substrate type, including primary and secondary terminal alkynyl alcohols, primary and secondary internal alkynyl alcohols, and primary terminal alkynyl alcohols having other functional groups. The present process proceeds cleanly at 25–130 °C and provides exocyclic enol ethers such as furans, pyrans, benzofurans, and isochromans in excellent conversion, high turnover frequencies, and regioselectivities. Mechanistic data implicate turnover-limiting insertion of C–C unsaturation into Ln–O bonds (involving a highly organized transition state) with subsequent, rapid Ln–C protonolysis. In addition, the reaction proceeds with an amino alkynyl alcohol in good selectivity for C–O bond formation.

Acknowledgment. Financial support by the NSF (Grant CHE-0809589) is gratefully acknowledged. We also thank Prof. R. J. Thomson (Northwestern University) for helpful discussions.

Supporting Information Available: Substrate characterization data. This material is available free of charge via the Internet at <http://pubs.acs.org>.

JA8072462

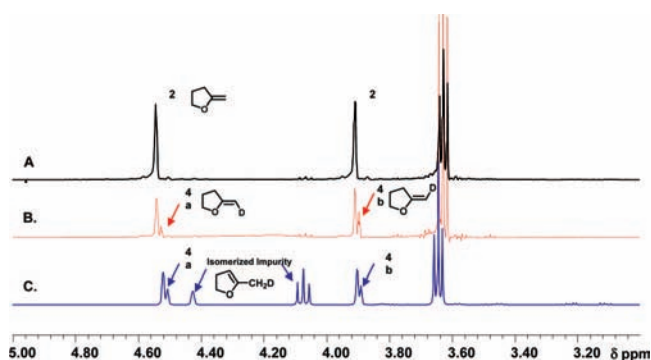


Figure 7. (A) Enlarged ^1H NMR spectrum (500 MHz) of product **2** in benzene- d_6 . (B) Enlarged ^1H NMR spectrum (500 MHz) of products **4a–c** and **2** in benzene- d_6 . (C) Enlarged ^1H NMR spectrum (500 MHz) of an authentic mixture of products **4a–c** and **2** in benzene- d_6 .